

False Discovery Rate Control via Data Splitting

Chenguang Dai^{*1}, Buyu Lin², Xin Xing¹, and Jun S. Liu¹

¹*Department of Statistics, Harvard University*

²*University of Science and Technology of China*

February 21, 2020

Abstract

Selecting relevant features associated with a given response variable is an important issue in many scientific fields. Quantifying quality and uncertainty of the selection via the false discovery rate (FDR) control has been of recent interest. This paper introduces a way of using data-splitting strategies to asymptotically control FDR for various feature selection techniques while maintaining high power. For each feature, the method estimates two independent significance coefficients via data splitting and constructs a contrast statistic. The FDR control is achieved by taking advantage of the statistic's property that, for any null feature, its sampling distribution is symmetric about 0. We further propose a strategy to aggregate multiple data splits (MDS) to stabilize the selection result and boost the power. Interestingly, this multiple data-splitting approach appears capable of overcoming the power loss caused by data splitting with FDR still under control. The proposed framework is applicable to canonical statistical models including linear models, Gaussian graphical models, and deep neural networks. Simulation results, as well as a real data application, show that the proposed approaches, especially the multiple data-splitting strategy, control FDR well and are often more powerful than existing methods including the Benjamini-Hochberg procedure and the knockoff filter.

1 Introduction

1.1 Motivation and background for the FDR control in regression models

Scientific researchers in the current big data era often have the privilege of collecting or accessing a large number of explanatory features targeting a specific response variable. For instance, population geneticists often need to profile thousands of single nucleotide polymorphisms (SNPs) in the genome-wide association study. A ubiquitous belief is that the response variable only depends on a small fraction of the collected features. Therefore, researchers are of primary interest to identify those relevant features, so that the computability of the downstream analysis, the reproducibility of the reported results, and the interpretability of the scientific findings can be largely enhanced. Throughout the article, we denote the explanatory features as (X_1, \dots, X_p) , with p being potentially large, and denote the response variable as y . We remark that this paper is presented in the context of feature selection (regression models), although all the methodological development can be possibly adapted to solve general multiple testing problems.

Many methodological contributions to the feature selection problem have been made by statisticians, including but not limited to stepwise regression, Lasso (Tibshirani, 1996), Dantzig selector (Candes and Tao, 2007), SCAD (Fan and Li, 2001), and some Bayesian methods (O'Hara and Sillanpää, 2009). A desired property of the selection procedure is the capability of controlling the number of false positives, which can be mathematically calibrated by the false discovery rate (FDR) (Benjamini and Hochberg, 1995) defined as below,

$$\text{FDR} = \mathbb{E}[\text{FDP}], \quad \text{FDP} = \frac{\#\{j : j \in S_0, j \in \widehat{S}\}}{\#\{j \in \widehat{S}\} \vee 1}, \quad (1)$$

^{*}The first two authors contributed equally to this paper.

where S_0 denotes the set of null features (irrelevant features), \widehat{S} denotes the set of selected features, and FDP refers to the false discovery proportion. The expectation is taken with respect to the randomness both in the data and in the selection procedure if it is not deterministic.

The first class of approaches is the Benjamin-Hochberg (BHq) procedure (Benjamini and Hochberg, 1995) and its extension, the Benjamin-Yekutieli (BYq) procedure (Benjamini and Yekutieli, 2001). BHq and BYq are only applicable when valid p-values are available for each feature. BHq guarantees an exact FDR control when all the p-values are independent, while BYq extends its applicability to the settings with dependent p-values. A further generalization of BHq, which is commonly referred to as the q-value approach, is detailed in Storey et al. (2004). The second class of approaches is the knockoff filter, including the fixed-design knockoff filter (Barber and Candès, 2015) and the model-X knockoff filter (Candès et al., 2018), which manages to control FDR by creating “knockoff” features in a similar spirit as the spike-ins in biological experiments. The knockoff filter does not require calculating individual p-values, and can be applied to fairly general settings without having to know the underlying true relationship between the response variable and the explanatory features. Further developments of the knockoff filter include the multilayer knockoff filter (Katsevich and Sabatti, 2019) and DeepPINK (Lu et al., 2018). More detailed discussions and comparisons of these methods are postponed to Section ?? after we introduce our method.

The third approach is the recently proposed Gaussian mirror method (Xin et al., 2019). Its essential idea is to perturb the features one by one and examine the corresponding impact. Specifically, for each feature X_j , the method creates a pair of perturbed mirror variables, $X_j^+ = X_j + c_j Z_j$ and $X_j^- = X_j - c_j Z_j$, where c_j is an adjustable scalar and Z_j follows $N(0, 1)$ independently, and constructs a statistic by contrasting the regression coefficients of the mirror variables obtained by the ordinary least squares (OLS) or Lasso. Their constructed statistic satisfies the property that its sampling distribution is symmetric about 0 if the underlying feature is a null feature, which is crucial to guarantee its asymptotic FDR control.

1.2 A review of data-splitting methods for the FDR control

We focus here on related data-splitting methods applicable to multiple testing problems (feature selection). Other applications of the data-splitting strategy include evaluating statistical predictions (cross validation) (Stone, 1974) and selecting efficient test statistics (Moran, 1973; Cox, 1975). In high-dimensional inference, a common practice of data splitting is to reduce the dimension of the problem. For linear models, two notable contributions are made by Wasserman and Roeder (2009) and Barber and Candès (2019). Wasserman and Roeder (2009) proposed to split the data into three parts to implement a three-stage regression method. In the first stage, the user fits a suite of candidate models to the data, with different tuning parameters, using the first part of the data. In the second stage, the second part of the data is used for selecting one of those models based on cross validations. In the third stage, null features are eliminated using hypothesis testing based on the third part of the data. Barber and Candès (2019) use the data-splitting strategy to extend the fixed-design knockoff framework to the high-dimensional setting. Specifically, the data is split into two parts, while the first part of data is used to screen out enough null features so that the fixed-design knockoff framework can be applied to the selected features on the second part of the data. We note that both methods rely on the so-called screening property, i.e., all relevant features are selected in the first step before the hypothesis testing or the knockoff filtering step. Moving beyond linear models, an assumption-free inference framework is proposed in Rinaldo et al. (2016) by combining data splitting and bootstrapping (or the normal approximation).

Another use of data splitting is to boost the power of multiple testing procedures. Two notable methods are proposed in Rubin et al. (2006) and Ignatiadis et al. (2016). Rubin et al. (2006) derive the optimal test statistic cutoffs that maximize the expected number of true positives, which depend on the underlying data generating process. The authors thus proposed to use data splitting, so that one part of the data is used to estimate the optimal cutoffs, while the rest of the data is used for testing. Ignatiadis et al. (2016) employ a hypothesis-weighting approach to improve the power of multiple testing. In particular, the authors proposed to use data splitting, in which one part of the data is used to determine proper weights for each individual hypotheses, and the other part of the data is used for large-scale multiple testing.

The undesirable randomness in data splitting can be lessened by repeating the procedure multiple times. Methodological developments along this line include methods proposed in van de Wiel et al. (2009), Meinshausen et al. (2009), and Romano and DiCiccio (2019), all of which aim at combining p-values obtained over multiple data splits. van de Wiel et al. (2009) proposed to aggregate p-values using the median, in testing the prediction error difference between two predictors constructed using each part of the data. A more sophisticated approach of combining p-values uses a properly scaled γ -quantile, as proposed in Meinshausen

et al. (2009), which gives asymptotic control of FDR under the screening property and an additional rank assumption on the design matrix. Romano and DiCiccio (2019) introduced several alternative approaches, based on concentration inequalities, or the limiting distribution of the averaged p-value. Our proposed approach is very different to the aforementioned methods, as it is built upon the inclusion rates estimated from multiple data splits rather than p-values.

1.3 Main contributions of the paper

In contrast to the Gaussian mirror method, which perturbs the data by adding and subtracting a Gaussian noise to each feature, we propose to impose a bootstrap-type perturbation via random data splitting, which is both conceptually simpler and computationally cheaper (can be done for all features simultaneously). Specifically, we split the whole data set into two halves, and apply two potentially different statistical learning procedures to each part of the data. The idea of using data splitting to make valid statistical inferences has been around for some time, and a review of related methods is given in Section 1.2. For most existing methods, the main motivation for splitting the data is to obtain valid p-values for each feature. Our proposed approach is different in the sense that, instead of aiming at p-values, we focus on perturbing the data to obtain two independent measurements of the importance of each feature so that a proper contrast between the two measurements of the same feature can be used to control FDR.

Ways of estimating the number of false positives without requiring p-values have been described in Barber and Candès (2015) for knockoff filters and Xin et al. (2019) for the Gaussian mirror method. The main idea is to construct a contrasting statistic M_j , called the “mirror statistic” in Xin et al. (2019), for each feature X_j , which enjoys the following two key properties as illustrated by Figure 1:

- (A1) A feature with a larger mirror statistic is more likely to be a relevant feature.
- (A2) The sampling distribution of the mirror statistic of a null feature is symmetric about 0.

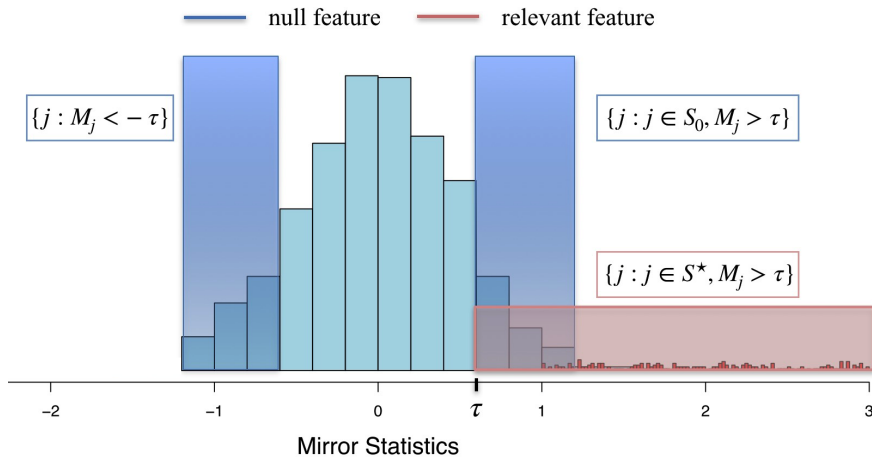


Figure 1: A cartoon illustration of the mirror statistic. M_j denotes the mirror statistic associated with feature X_j . S_0 denotes the set of null features, and S^* denotes the set of relevant features. Features associated with a mirror statistic larger than the cutoff τ are selected.

Property (A1) suggests that we can rank the importance of each feature by its mirror statistic, and select those features with their mirror statistics greater than a cutoff value (τ in Figure 1). Property (A2) implies that we can estimate (conservatively) the number of false positives $\#\{j : j \in S_0, M_j > \tau\}$ by $\#\{j : M_j < -\tau\}$, if the mirror statistics of the null features are not too correlated. Based upon this principle, given any FDR control level $q \in (0, 1)$, we can choose a data-driven cutoff τ_q so that our proposed approach can achieve an asymptotic FDR control. As we will see, Property (A1) is naturally satisfied due to the construction of the mirror statistic, thus our main concern is Property (A2).

Another main contribution of this work is to propose a multiple data-splitting (MDS) approach, which both reduces the variability of the selection result and boosts the power. For the ease of presentation, we refer to the single data-splitting approach and the multiple data-splitting approach as DS and MDS, respectively. Instead of ranking the features by the mirror statistics, we rank them by their inclusion rates estimated

through multiple data splits. We show that FDR can be still under control if the rank of the inclusion rate is reasonably consistent with the rank of the feature importance. Empirically, we observe that MDS has the capability to almost retrieve the full power without splitting the data. We back up the empirical result by studying a simple Normal mean model, and we prove that the inclusion rate is a monotone decreasing function of the p-value calculated using the full data set. In particular, MDS can be regarded as a Rao-Blackwell improvement of DS in terms of ranking the features.

We apply the data-splitting approaches to three canonical models including the linear model, the Gaussian graphical model, and the deep neural network. For the linear model, we focus on the high-dimensional setting, in which two strategies are considered. The simpler strategy is to first select preliminary features using one part of the data via a high-dimensional feature selection procedure such as Lasso, and then run OLS on the selected features using the other part of the data. The more involved strategy aims at directly symmetrizing the Lasso estimator using the post-selection inference theory (Lee et al., 2016). Property (A2) is satisfied if all relevant features are selected in the first step (the so-called screening property).

Methods designed for the linear model are applicable to the Gaussian graphical model because of the linear representation of the conditional dependence structure (Lauritzen, 1996). Given an FDR control level q , we apply DS or MDS to each nodewise linear regression with designated FDR control level $q/2$, and then combine the nodewise selection results using the OR rule (Meinshausen and Bühlmann, 2006). Our simulation study shows that DS and MDS performed significantly better than existing approaches including BHq based on the partial correlation test and GFC proposed in Liu (2013).

For the deep neural network, we train two identically structured networks using each part of the data. Two types of mirror statistics are considered in order to cope with the issue of non-identifiability of labels of the hidden units in each network. The first one is built on weight multiplications as in Lu et al. (2018), while the second one utilizes the influence function (Hechtlinger, 2016) to measure each feature’s importance. The influence function approach appears to be also applicable to more sophisticated networks including convolutional and recurrent neural networks. For the fully-connected feed-forward neural networks, the performances of the two approaches are similar based on our empirical studies.

The rest of the paper is structured as follows. Section 2.1 introduces DS, a proposed FDR control approach based on a single data split. Section 2.2 and 2.3 detail MDS, accompanied by useful theoretical insights on a simple Normal means model. Section 2.4 compares our approaches with existing methods including BHq, the knockoff filter, and the Gaussian mirror method. Section 3 discusses the applications of the proposed data-splitting approaches on three popular models including the linear model, the Gaussian graphical model, and the deep neural network model. Section 4 demonstrates the competitive performances of DS and MDS through simulation studies on the aforementioned models. Section 4.4 applies DS and MDS to the task of identifying mutations associated with drug resistance in the HIV-1 data. Section 5 concludes with a few final remarks.

2 Data Splitting for the FDR Control

2.1 Single data split

Suppose there is a set of random features $\{X_1, \dots, X_p\}$, which jointly follow some p -dimensional probability distribution. Denote the n independent observations of these features as $\mathbf{X}_{n \times p} = (\mathbf{X}_1, \dots, \mathbf{X}_p)$, also known as the *design matrix*. The bold case $\mathbf{X}_j = (X_{1j}, \dots, X_{nj})^\top$ denotes the vector containing n independent realizations of feature X_j . For each set of observed features (X_{i1}, \dots, X_{ip}) , there is an associated response variable y_i , for $i \in [n]$. Let $\mathbf{y} = (y_1, \dots, y_n)^\top$ be the vector of n independent responses. For each subset S of $\{1, \dots, p\}$, we denote $X_S = \{X_j : j \in S\}$ and $X_{-S} = \{X_j : j \notin S\}$. The task of variable or feature selection is to find the smallest set S^* such that

$$y \perp\!\!\!\perp X_{-S^*} \mid X_{S^*}.$$

In the following, we denote S^* as the set of indexes for relevant features (non-null features). Thus, $S_0 = \{1, \dots, p\} \setminus S^*$ is the complementary set of indexes, and $X_{S_0} = X_{-S^*}$ is the collection of all null features. In practice, one should first de-mean and standardize the features *a priori* so as to make the features comparable to each other. Let $p_0 = |S_0|$ and $p_1 = |S^*|$ be the number of null features and relevant features, respectively.

The selection of relevant features for a statistical learning model such as regression commonly relies on a set of coefficients (or other measures of “impact”) $\{\hat{\beta}_1, \dots, \hat{\beta}_p\}$, each corresponding to one feature, which are estimated based on the observed data. The larger the $|\hat{\beta}_j|$ is, the more likely we believe that feature X_j is useful in predicting y . For example, in the linear regression setting, $\hat{\beta}_j$ can be the regression coefficient

estimated via OLS or Lasso. Contrast to the commonly practiced approaches that select features based on a single coefficient estimate $\widehat{\beta}_j$ for each feature X_j , we propose to construct two independent estimates of the coefficient, $\widehat{\beta}_j^{(1)}$ and $\widehat{\beta}_j^{(2)}$, potentially with two different statistical procedures, in order to set up an FDR control framework.

The independence of the two coefficient estimates can be ensured by employing a data-splitting strategy. To be specific, we split the n observations into two groups, denoted as $(\mathbf{y}^{(1)}, \mathbf{X}^{(1)})$ and $(\mathbf{y}^{(2)}, \mathbf{X}^{(2)})$. Then, we obtain $\widehat{\beta}_j^{(1)}$ based on $(\mathbf{y}^{(1)}, \mathbf{X}^{(1)})$, and $\widehat{\beta}_j^{(2)}$ based on $(\mathbf{y}^{(2)}, \mathbf{X}^{(2)})$. We note that the data-splitting procedure can be arbitrary, not necessary to be completely at random. The sample sizes for the two groups can also be different. The only requirement is that it should be independent of the response variables \mathbf{y} , which can be easily satisfied if we split the data without looking at \mathbf{y} .

Motivated by [Xin et al. \(2019\)](#), we construct feature X_j 's *mirror statistic* as

$$M_j = \left| \widehat{\beta}_j^{(1)} + \widehat{\beta}_j^{(2)} \right| - \left| \widehat{\beta}_j^{(1)} - \widehat{\beta}_j^{(2)} \right|. \quad (2)$$

Given a designated FDR control level $q \in (0, 1)$, the goal is to choose a data-dependent cutoff τ_q , so that FDR among the selected features $\{j : M_j > \tau_q\}$ is under q . To achieve this asymptotically, we need to impose a few essential requirements on the M_j 's for both relevant and null features. For a relevant feature, its M_j tends to be large if (i) $\widehat{\beta}_j^{(1)}$ and $\widehat{\beta}_j^{(2)}$ have the same sign; (ii) $|\widehat{\beta}_j^{(1)}|$ and $|\widehat{\beta}_j^{(2)}|$ are both relatively large. For a null feature, we require the following assumption on the sampling distribution of either $\widehat{\beta}_j^{(1)}$ or $\widehat{\beta}_j^{(2)}$ to control FDR. Without loss of generality, we state the assumption in terms of $\widehat{\beta}_j^{(2)}$.

Assumption 1 (*Symmetric Assumption*) *For each null feature index $j \in S_0$, conditioning on the design matrix $\mathbf{X}^{(2)}$, the sampling distribution of $\widehat{\beta}_j^{(2)}$ is symmetric about 0.*

We note that (i) the symmetric assumption is only imposed on null features, and is not required for relevant features; (ii) for the purpose of FDR control, it is sufficient that either $\widehat{\beta}_j^{(1)}$ or $\widehat{\beta}_j^{(2)}$ satisfies the symmetric assumption. We will show that the symmetric assumption can be satisfied with high probability for some standard statistical models, such as the linear model and the Gaussian graphical model, under some proper conditions. For more general statistical learning models, there is no guarantee for the symmetric assumption, although empirically we find that our proposed approach can be applied effectively to complex models such as fully connected deep neural networks. A detailed discussion of the symmetric assumption for different statistical models is deferred to [Section 3](#). We have the following property for the mirror statistics:

Lemma 1 *Under [Assumption 1](#), regardless of the data-splitting procedure, the sampling distribution of M_j is symmetric about 0 for each $j \in S_0$.*

The proof is elementary and thus omitted. The simultaneous symmetric property of the mirror statistics for null features leads us to approximately upper bound the number of false discoveries as follows:

$$\#\{j \in S_0 : M_j > t\} \approx \#\{j \in S_0 : M_j < -t\} \leq \#\{j : M_j < -t\}, \quad \forall t > 0.$$

Therefore, an over-estimated FDP of our selection $\widehat{S}_t = \{j : M_j > t\}$ is

$$\widehat{\text{FDP}}(t) = \frac{\#\{j : M_j < -t\}}{\#\{j : M_j > t\} \vee 1}.$$

For any designated FDR control level q , we can choose the data-driven cutoff τ_q as follows:

$$\tau_q = \min\{t > 0 : \widehat{\text{FDP}}(t) \leq q\}, \quad (3)$$

and our final selection will be $\widehat{S}_{\tau_q} = \{j : M_j > \tau_q\}$. A summary of our proposed method can be found in [Algorithm 1](#). To prove that the procedure asymptotically control FDR under a pre-specified level q as $p \rightarrow \infty$, we require the following weak dependency assumption for all the mirror statistics associated with the null features.

Assumption 2 (*Weak dependency*) *The mirror statistics M_j 's are continuous random variables, and there exist constants $C > 0$ and $\alpha \in (0, 2)$ such that*

$$\text{Var} \left(\sum_{j \in S_0} \mathbb{1}(M_j > t) \right) \leq Cp_0^\alpha, \quad \forall t \in \mathbb{R}.$$

To understand this assumption, we note that if the mirror statistics M_j 's, associated with the null features, are perfectly correlated, or can be clustered into a fixed number of groups so that their within-group correlation is 1, then α has to be 2 and the assumption does not hold. However, if the dependence between M_j and M_{j+k} decays at a reasonable rate of k , Assumption 2 holds. Under this assumption, the proposition below justifies our proposed approach for controlling FDR.

Proposition 1 *For any given FDR control level q , under Assumptions 1 and 2, if $p_0 \rightarrow \infty$ as $p \rightarrow \infty$, we have*

$$\mathbb{E} \left[\frac{\#\{j : j \in S_0, j \in \widehat{S}_{\tau_q}\}}{\#\{j : j \in \widehat{S}_{\tau_q}\} \vee 1} \right] \leq q \quad \text{as } p \rightarrow \infty.$$

The proof of Proposition 1 is postponed to the Appendix.

Algorithm 1 False discovery rate control via single data split

1. Split the data set into two groups $(\mathbf{y}^{(1)}, \mathbf{X}^{(1)})$ and $(\mathbf{y}^{(2)}, \mathbf{X}^{(2)})$, independent of the response variable \mathbf{y} .
2. Estimate the ‘‘impact’’ coefficients on each part of the data to obtain $\widehat{\beta}_j^{(1)}$ and $\widehat{\beta}_j^{(2)}$ for $j \in [p]$. The two estimation procedures can be potentially different.
3. Calculate the mirror statistics $M_j = \left| \widehat{\beta}_j^{(1)} + \widehat{\beta}_j^{(2)} \right| - \left| \widehat{\beta}_j^{(1)} - \widehat{\beta}_j^{(2)} \right|$ for $j \in [p]$.
4. Given a designated FDR level $q \in (0, 1)$, calculate the cutoff τ_q as below:

$$\tau_q = \min \left\{ t > 0 : \widehat{\text{FDP}}(t) = \frac{\#\{j : M_j < -t\}}{\#\{j : M_j > t\} \vee 1} \leq q \right\}.$$

5. Select the features $\{j : M_j > \tau_q\}$.
-

2.2 Multiple data splits

There are two major concerns about the single data-splitting procedure (DS). First, splitting the data into two halves inflates the variances of the estimated coefficients, thus the procedure can potentially suffer from a power loss. Second, the selection result is not stable and can vary substantially across different data splits. A natural way to remedy these issues is to repeat the procedure multiple times and appropriately aggregate the selection results. In the settings when p-values are available, Meinshausen et al. (2009) proposed a method to aggregate the dependent p-values obtained from multiple sample splits. We here propose a different approach, detailed in Algorithm 2, to aggregate multiple selection results without requiring p-values, which can almost achieve the power of using the full data.

Suppose we repeat the data-splitting procedure m times independently. Each time the set of selected features is denoted as $\widehat{S}^{(k)}$, $k \in [m]$. For each feature X_j , we define its population inclusion rate I_j and the corresponding empirical inclusion rate \widehat{I}_j as

$$I_j = \mathbb{E} \left[\frac{\mathbb{1}(j \in \widehat{S})}{|\widehat{S}| \vee 1} \right], \quad \widehat{I}_j = \frac{1}{m} \sum_{k=1}^m \frac{\mathbb{1}(j \in \widehat{S}^{(k)})}{|\widehat{S}^{(k)}| \vee 1}, \quad (4)$$

where the expectation is taken with respect to both the randomness in \mathbf{y} and the randomness in data splitting. The proposed aggregation approach is most useful if the following informal statement is approximately true: if a feature is selected less frequently in the m independent data splits, it is less likely to be a relevant feature. In other words, the rank of each feature in terms of the inclusion rate should roughly reflect the feature’s importance. If this holds, we only need to choose a inclusion rate cutoff so that the features with their inclusion rates greater than the cutoff are selected.

Our intuition is based on the fact that conditioning on the design matrix \mathbf{X} , if we can regenerate m independent sets of the response variable \mathbf{y} and apply the proposed method, on average, the false discovery proportions should be (asymptotically) no larger than q based on Proposition 1. Although there is no way for

us to regenerate data, we propose a backtracking procedure based on this fact, by treating the m dependent selection results obtained from repeated data splits as an approximation to m independent selection results obtained with data regeneration.

Specifically, we first sort the features with respect to their empirical inclusion rates in an increasing order. Denote the sorted inclusion rates as $0 \leq \widehat{I}_{(1)} \leq \widehat{I}_{(2)} \leq \dots \leq \widehat{I}_{(p)}$. The cutoff is then chosen to be the largest $\ell \in [p]$ such that $\widehat{I}_{(1)} + \dots + \widehat{I}_{(\ell)} \leq q$. A heuristic justification for this selection is as follows. Imagine that the set of features $\{j : \widehat{I}_j > \widehat{I}_{(\ell)}\}$ are all relevant features, and the set of features $\{j : \widehat{I}_j \leq \widehat{I}_{(\ell)}\}$ are all null features. Then, if we review the m selection results, we can find that the average false discovery proportions of the m data-splitting selection procedures is the largest under q .

Algorithm 2 Aggregating selection results from multiple data splits

1. Sort the features with respect to their empirical inclusion rates in an increasing order. Denote the sorted empirical inclusion rates as $0 \leq \widehat{I}_{(1)} \leq \widehat{I}_{(2)} \leq \dots \leq \widehat{I}_{(p)}$.
 2. Find the largest $\ell \in [p]$ such that $\widehat{I}_{(1)} + \dots + \widehat{I}_{(\ell)} \leq q$.
 3. Select the features $\widehat{S} = \{j : \widehat{I}_j > \widehat{I}_{(\ell)}\}$.
-

In terms of the FDR control, we provide a theoretical justification of the multiple data-splitting (MDS) approach at the population level. That is, we proceed as if we have access to the population inclusion rate I_j for $j \in [p]$, where in practice, the empirical inclusion rate \widehat{I}_j serves as an unbiased estimator to I_j . We require the following assumptions.

Assumption 3 (a) (Null exchangeability) *The distribution of $\{\mathbb{1}(j \in \widehat{S}), j \in S_0\}$ is exchangeable.*

(b) (Rank faithfulness) *For any $\alpha \in (0, 1)$, we have*

$$\limsup_{p \rightarrow \infty} \frac{1}{p_1} \sum_{j \in S^*} \mathbb{1}\left(I_j \leq \frac{\alpha}{p_0}\right) \leq \alpha,$$

where $p_0 = |S_0|$, $p_1 = |S^*|$.

(c) (Procedure faithfulness) *For each single data split, the procedure has an asymptotic FDR control, that is,*

$$\limsup_{p \rightarrow \infty} \mathbb{E} \left[\frac{\#\{j : j \in S_0, j \in \widehat{S}\}}{\#\{j : j \in \widehat{S}\} \vee 1} \right] = \limsup_{p \rightarrow \infty} \sum_{j \in S_0} I_j \leq q.$$

Assumption 3(a) also appears in [Meinshausen and Bühlmann \(2010\)](#) (Theorem 1), and it directly implies that for any $i, j \in S_0$, $I_i = I_j$. Assumption 3(b) guarantees that the rank of a feature, in terms of the inclusion rate, is more informative of the feature's importance than random guessing. Under Assumption 3, we have the following proposition.

Proposition 2 *For any FDR control level $q \in (0, 1)$, let ℓ be the largest value in $[p]$ such that $I_{(1)} + \dots + I_{(\ell)} \leq q$, in which $0 \leq I_{(1)} \leq I_{(2)} \leq \dots \leq I_{(p)}$ are the order statistics of the population inclusion rates. Under Assumption 3, we have*

$$\limsup_{p \rightarrow \infty} \frac{\sum_{j \in S_0} \mathbb{1}(I_j > I_{(\ell)})}{\sum_{j=1}^p \mathbb{1}(I_j > I_{(\ell)}) \vee 1} \leq q, \tag{5}$$

in the asymptotic regime $p_0 \rightarrow \infty$ and $\liminf_{p \rightarrow \infty} p_1/p_0 > 0$.

The proof can be found in the Appendix.

2.3 A theoretical study of MDS for the Normal means model

We next consider a simple Normal means model, upon which we show that MDS can achieve almost the full power without splitting the data. For $i \in [n]$, we assume X_{ij} follow $N(\mu_j, \sigma^2)$, where $j \in [p]$ and σ^2 is known. We assume all X_{ij} are independent. To test whether μ_j is 0, the standard p-value is given by $p_j = \Phi(-|\sqrt{n}\bar{X}_j/\sigma|)$, where $\bar{X}_j = \sum_{i=1}^n X_{ij}/n$, and Φ is the CDF of the standard Normal distribution. Under this setup, we have the following proposition.

Proposition 3 *For the Normal means model described above, the population inclusion rate defined in Equation (4) is monotone with respect to the p-value calculated using the full data. Mathematically, this means*

$$\mathbb{E} \left[\frac{\mathbb{1}(j \in \hat{S})}{|\hat{S}| \vee 1} \middle| p_j \right]$$

is a monotone decreasing function of p_j for all $j \in [p]$.

The proof is postponed to the Appendix.

Proposition 3 implies that for this simple model, the rank of the features, in terms of the inclusion rates, can be as informative as the rank in terms of p-values. Therefore, if the empirical inclusion rate \hat{I}_j is a reasonable estimate to the population inclusion rate I_j , MDS is possibly as powerful as those methods based on the rank of p-values, which are calculated using the full data set.

Proposition 3 also suggests why MDS is superior to DS in terms of ranking the features. For DS, we can substitute the ranks by the mirror statistics with the ranks by $\mathbb{1}(j \in \hat{S})/(|\hat{S}| \vee 1)$, which does not decrease the number of correctly ranked pairs. That is, for any pair of feature indexes (i, j) , if the rank by the mirror statistics aligns with the rank by the p-values, say $p_i \leq p_j$ and $M_i \geq M_j$, then the rank by $\mathbb{1}(j \in \hat{S})/(|\hat{S}| \vee 1)$ also aligns with the rank by the p-values, i.e., $\mathbb{1}(i \in \hat{S})/(|\hat{S}| \vee 1) \geq \mathbb{1}(j \in \hat{S})/(|\hat{S}| \vee 1)$. For MDS, all the features are ranked by $\mathbb{E}[\mathbb{1}(j \in \hat{S})/(|\hat{S}| \vee 1) | \mathbf{X}]^1$, where the expectation is taken with respect to the randomness in data splitting. In this simple model, MDS yields a rank better aligned with the rank of p-values, because conditioning on the p-values,

$$\text{Var} \left(\frac{\mathbb{1}(j \in \hat{S})}{|\hat{S}| \vee 1} \right) \geq \text{Var} \left(\mathbb{E} \left[\frac{\mathbb{1}(j \in \hat{S})}{|\hat{S}| \vee 1} \middle| \mathbf{X} \right] \right),$$

where the variance on the left hand side is taken with respect to both the randomness in the data and the randomness in data splitting, while the variance on the right hand side is taken with respect to the randomness only in the data. Therefore, MDS is essentially a Rao-Blackwell improvement of DS.

We empirically check Assumption 3(b) and Proposition 3 on the Normal means model. We set $\sigma = 1$, $p = 800$, $p_1 = 160$, $n = 1000$, and $m = 400$. For $j \in [p_1]$, μ_j is sampled from $N(0, \delta^2)$, whereas the rest μ_j 's are set to be 0. The left panel of Figure 2 shows that Assumption 3(b) is satisfied for various signal strengths $\delta = 0.1, 0.2, 1$, in which the red line represents the upper bound αp_1 , and the other three lines represent the number of less-frequently selected relevant features, $\sum_{j \in S^*} \mathbb{1}(I_j \leq \alpha/p_0)$. In the right panel of Figure 2, we set $\delta = 0.5$, and plot the empirical inclusion rates (red “*”) and the mirror statistics based on a single split (blue “+”) against the p-values calculated using the full data set. We see that the empirical inclusion rate is approximately a monotone decreasing function of the p-value. Besides, the rank of the empirical inclusion rates aligns better with the rank of the p-values, and is much more informative than the rank of the mirror statistics.

2.4 Comparison with existing methods

The proposed data-splitting methods are perhaps most useful in the settings when practicing exact or asymptotic hypothesis testing is not straightforward. That is, a valid p-value from the significance test for each feature is not available, upon which some popular FDR control procedures rely, including BHq, BYq, and the q-value approach.

The high-dimensional linear model serves as a canonical example where constructing valid p-values is difficult. Much effort has been made in the literature for obtaining valid p-values for the selected features using

¹In more general cases where we conditioning on the design matrix \mathbf{X} and the randomness comes from the response variable \mathbf{y} , MDS ranks all the features by $\mathbb{E}[\mathbb{1}(j \in \hat{S})/(|\hat{S}| \vee 1) | \mathbf{y}]$.

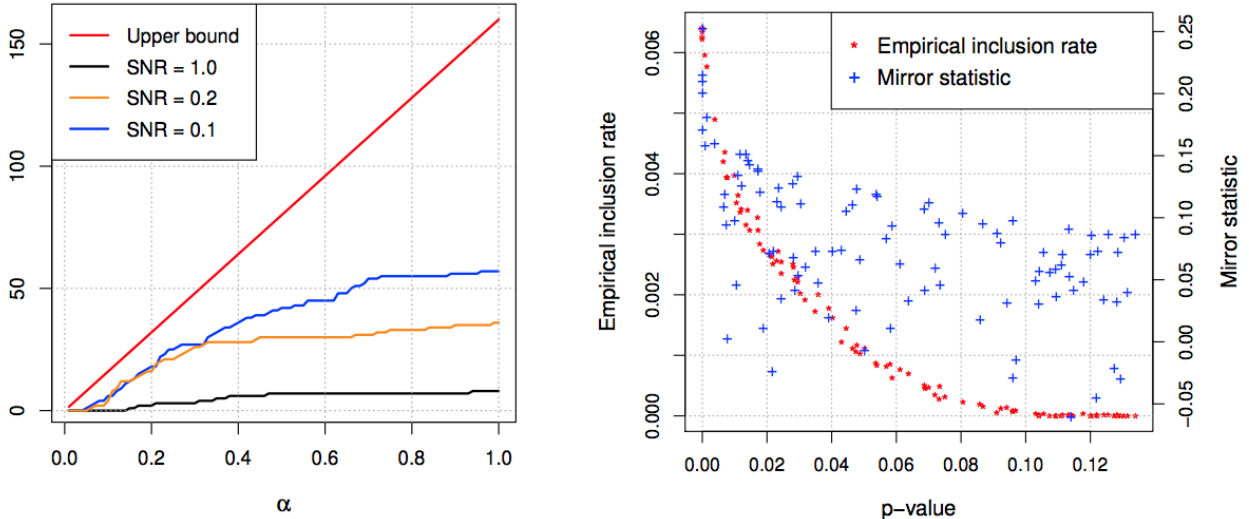


Figure 2: (Left) Check of Assumption 3(b). The red line represents the upper bound αp_1 , while the other three lines represent the number of less-frequently selected relevant features, $\sum_{j \in S^*} \mathbb{1}(I_j \leq \alpha/p_0)$, under different signal-to-noise ratios (SNR) $\{0.1, 0.2, 1\}$, respectively. (Right) Empirical inclusion rates and mirror statistics against p-values calculated using the full data set.

the theory of post-selection inference. Popular selection procedures including Lasso (Lee et al., 2016), forward stepwise regression, and least angle regression (Tibshirani et al., 2016) have been considered. However, this type of theory is mostly developed case by case, and can not be easily generalized to other selection procedures such as SCAD (Fan and Li, 2001) and elastic net (Zou and Hastie, 2005). DS and MDS are more flexible in the sense that as long as the screening property holds, i.e., all the relevant features are estimated to be nonzero in $\hat{\beta}^{(1)}$ (see Section 3.1), the selection result enjoys an asymptotic FDR control.

The knockoff filter is another class of methods that provides an exact FDR control without requiring p-values. The fixed-design knockoff filter (Barber and Candès, 2015) is proposed to exactly control FDR for the linear model in low-dimensional settings ($n \geq 2p$). The model-X knockoff filter (Candès et al., 2018) largely generalizes its applicability to arbitrary models between y and X in high-dimensional settings. The knockoff filter is theoretically superior to DS and MDS in the sense that it guarantees a finite sample FDR control instead of an asymptotic FDR control. However, DS and MDS can be more favorable from the following perspectives. First, in high-dimensional settings, the model-X knockoff filter is only applicable if the joint distribution of all the features is known, otherwise estimating the joint distribution itself can be very challenging. Because DS and MDS require no knowledge of the feature generating process, they are expected to be more robust in real applications. Second, DS and MDS are computationally more efficient compared to the model-X knockoff filter because generating knockoff features in high-dimensional settings can be quite expensive. Third, empirically we find that when the features are highly correlated, the model-X knockoff filter can be too conservative to detect relevant features (see Section 4.1).

The proposed data-splitting approaches are also computationally more favorable compared to the Gaussian mirror method (Xin et al., 2019). For the linear model, the Gaussian mirror method requires running p times linear fittings, whereas DS and MDS only requires running 2 and $2m$ linear fittings, respectively, which can be much smaller than p . For the Gaussian graphical model, DS requires running $2p$ times nodewise linear fittings (see Section 3.2). The Gaussian mirror method is also potentially applicable to the Gaussian graphical model. However, it requires p^2 times nodewise linear fittings, which is unacceptable in high-dimensional settings unless using parallel computing resources.

3 Specializations for Different Statistical Models

In this section, we discuss how we construct the “impact” coefficients for several popular statistical models. Our main concern is that the “impact” coefficient $\hat{\beta}^{(2)}$, calculated based on $(\mathbf{y}^{(2)}, \mathbf{X}^{(2)})$, shall satisfy the symmetric assumption (Assumption 1). We assume that the data-splitting procedure is done so that the discussion throughout this section is conditioning on the data-splitting result.

3.1 Linear model

The linear model assumes that the true data generating process is $\mathbf{y} = \mathbf{X}\boldsymbol{\beta}^* + \boldsymbol{\epsilon}$, where $\boldsymbol{\beta}^*$ denotes the true regression coefficient, and the noise $\boldsymbol{\epsilon}$ follows $N(\mathbf{0}, \sigma^2 \mathbf{I}_n)$. In the context of feature selection, $\boldsymbol{\beta}^*$ is often assumed to be nonzero restricted on a subset $S^* \subseteq \{1, \dots, p\}$. In the low-dimensional setting where \mathbf{X} is full rank ($n \geq p$), we can simply run the ordinary least regression (OLS), and take the estimated regression coefficient as the ‘‘impact’’ coefficient $\widehat{\boldsymbol{\beta}}^{(2)}$. Because the sampling distribution of $\widehat{\boldsymbol{\beta}}^{(2)}$, with respect to the randomness in $\mathbf{y}^{(2)}$, is $N(\boldsymbol{\beta}^*, \sigma^2 (\mathbf{X}^{(2)\top} \mathbf{X}^{(2)})^{-1})$, the symmetric assumption is satisfied. $\widehat{\boldsymbol{\beta}}^{(1)}$ can be estimated using either OLS or any other regularization methods such as Lasso.

In the high-dimensional setting where $p > n$, we consider two approaches, both of which rely on the so-called screening property. The screening property means that after applying some feature selection method to $(\mathbf{X}^{(1)}, \mathbf{y}^{(1)})$, the selected feature set contains all the relevant features, that is, $\widehat{S}^{(1)} \supseteq S^*$. For Lasso, under the restricted eigenvalue condition (Bickel et al., 2009), which rules out the scenario that the design matrix has unacceptably high pairwise correlation, and the ‘‘beta-min’’ condition (Dezeure et al., 2015), which ensures that the signal strength is large enough, the screening property holds with high probability. We remark that the ‘‘beta-min’’ condition calibrates the minimum requirement for the signal strength as a function of $p_1 = |S^*|$ and p , thus it does not contradict Assumption 2.

The first approach still uses OLS to construct the ‘‘impact’’ coefficient $\widehat{\boldsymbol{\beta}}^{(2)}$, but on the subset of features $\widehat{S}^{(1)}$, selected using the first half of data $(\mathbf{y}^{(1)}, \mathbf{X}^{(1)})$. The symmetric assumption holds for $\widehat{\boldsymbol{\beta}}^{(2)}$ as long as the screening property holds for $\widehat{\boldsymbol{\beta}}^{(1)}$. In the following, we refer to the procedure, which applies Lasso to $(\mathbf{X}^{(1)}, \mathbf{y}^{(1)})$ and OLS to $(\mathbf{X}^{(2)}, \mathbf{y}^{(2)})$, as the Lasso + OLS procedure.

The second approach is built on the theory of post-selection inference developed in recent years. We aim at directly symmetrizing $\widehat{\beta}_j^{(1)}$ for $j \in S_0$, under the assumption that the screening property holds for $\widehat{\boldsymbol{\beta}}^{(1)}$. In the following, we assume that $\widehat{\boldsymbol{\beta}}^{(1)}$ is estimated using Lasso, while alternative methods including stepwise procedures (Taylor et al., 2014) can be considered similarly. We also assume that the noise level σ^2 is known. We note that it is sufficient for us to only symmetrize $\widehat{\beta}_j^{(1)}$ with $j \in \widehat{S}^{(1)}$, because the rest of the features won’t be selected using our procedure as their associated mirror statistics are 0. The symmetrization mainly contains the following two steps, based on Theorem 5.2 in Lee et al. (2016).

1. Update $\widehat{\beta}_j^{(1)}$ for all $j \in \widehat{S}^{(1)}$ by refitting an OLS on $(\mathbf{X}^{(1)}, \mathbf{y}^{(1)})$, only using the features selected in $\widehat{S}^{(1)}$.
2. For each $j \in \widehat{S}^{(1)}$, transform $\widehat{\beta}_j^{(1)}$ to $F_{0, \sigma_j^2}^{[a_j, b_j]}(\widehat{\beta}_j^{(1)}) - 1/2$, where $F_{\mu, \sigma^2}^{[a, b]}$ denote the CDF of the truncated normal distribution truncated to the interval $[a, b]$, with mean μ and variance σ^2 . The formulas for σ_j^2, a_j, b_j essentially follow from Lee et al. (2016), thus are detailed in the Appendix.

We note that for $j \in S_0$, $F_{0, \sigma_j^2}^{[a_j, b_j]}(\widehat{\beta}_j^{(1)}) - 1/2$ follows $\text{Unif}(-1/2, 1/2)$. Therefore the symmetric assumption is satisfied. $\widehat{\boldsymbol{\beta}}^{(2)}$ can be transformed similarly.

Empirically, we find that the first approach is more robust than the second one, except for the case where the design matrix has very high pairwise partial correlation, leading to a variance inflation of the OLS estimates. We also observe some power loss for the second approach. The reason is that for the relevant feature $j \in S^*$, the mean of the corresponding truncated normal distribution is not 0, but β_j^* . Therefore, the transformation is not sensible to the regression coefficients of the relevant features, and can unintentionally distort useful signals.

3.2 Gaussian graphical model

Suppose $\mathbf{X} = (X_1, \dots, X_p)$ follows a p -dimensional multivariate normal distribution $N(\boldsymbol{\mu}, \Sigma)$ with $\Sigma = (\sigma_{ij})$. Without loss of generality, we assume $\boldsymbol{\mu} = \mathbf{0}$. One can define a corresponding Gaussian graphical model (V, E) , in which the set of vertexes is $V = (X_1, \dots, X_p)$, and there is an edge between two different vertexes X_i and X_j if X_i and X_j are conditionally independent, that is, $X_i \perp\!\!\!\perp X_j | \{X_k, k \neq i, j\}$. The estimation of the graphical structure is equivalent to the selection of the precision matrix $\Lambda = \Sigma^{-1} = (\lambda_{ij})$. For each vertex X_j , we can write $X_j = \mathbf{X}_{-j}^\top \boldsymbol{\beta}^j + \epsilon_j$, in which ϵ_j (independent of \mathbf{X}_{-j}) follows a centered normal distribution, and $\boldsymbol{\beta}^j = -\lambda_{jj}^{-1} \boldsymbol{\Lambda}_{j, -j}$. Therefore, $\lambda_{i,j} = 0$ implies that X_i and X_j are conditionally independent. Let the neighborhood of each vertex X_j be $ne_j = \{k \in [p] : k \neq j, \beta_k^j \neq 0\}$, and its complement be $ne_j^c = \{k \in [p] : k \neq j, \beta_k^j = 0\}$.

Given i.i.d samples $\mathbf{X}_1, \dots, \mathbf{X}_n$ from $N(\boldsymbol{\mu}, \Sigma)$, it is natural to consider first recovering the support of each β^j using feature selection methods such as Lasso (Meinshausen and Bühlmann, 2006), then combining all the nodewise selection results properly to estimate the global graph structure. In view of this, we propose an FDR control approach, with a designated FDR control level q , for the estimation of Gaussian graphical models. The proposed method mainly contains the following two steps:

1. Apply the proposed data-splitting approaches for linear models (see Section 3.1) to each nodewise edge selection, with designated FDR control level $q/2$. Denote the nodewise selection results as $\widehat{ne}_j = \{k \in [p] : k \neq j, \widehat{\beta}_k^j \neq 0\}$ for $j \in [p]$.
2. Combine the nodewise selection results using the OR rule to estimate the graph structure:

$$\widehat{E}_{\text{OR}} = \{(i, j) \in [p] \times [p], i \in \widehat{ne}_j \text{ or } j \in \widehat{ne}_i\}. \quad (6)$$

A heuristic justification of the proposed approach is given as below:

$$\begin{aligned} \text{FDP} &= \frac{\#\{(i, j) \in \widehat{E}_{\text{OR}}, (i, j) \notin E\}}{|\widehat{E}_{\text{OR}}| \vee 1} \leq \frac{\sum_{j=1}^p \#\{i \in ne_j^c, i \in \widehat{ne}_j\}}{\frac{1}{2} \sum_{j=1}^p \#\{i \in \widehat{ne}_j\} \vee 1} = \frac{\sum_{j=1}^p \#\{i \in ne_j^c, M_{ji} > \tau_{q/2}^j\}}{\frac{1}{2} \sum_{j=1}^p \#\{M_{ji} > \tau_{q/2}^j\} \vee 1} \\ &\approx \frac{\sum_{j=1}^p \#\{i \in ne_j^c, M_{ji} < -\tau_{q/2}^j\}}{\frac{1}{2} \sum_{j=1}^p \#\{M_{ji} > \tau_{q/2}^j\} \vee 1} \leq 2 \max_{j \in [p]} \frac{\#\{i \in ne_j^c, M_{ji} < -\tau_{q/2}^j\}}{\#\{M_{ji} > \tau_{q/2}^j\} \vee 1} \leq q. \end{aligned} \quad (7)$$

For $j \in [p]$, $\tau_{q/2}^j$ is the cutoff of the mirror statistics in the nodewise edge selection of the vertex X_j , and M_{ji} is the mirror statistic associated with X_i for $i \in [p] \setminus \{j\}$. The first inequality is based on the fact that each edge can be selected at most twice. The approximation in the middle utilizes the symmetric property of the mirror statistics. The second to last inequality comes from the elementary inequality $\sum_n a_n / \sum_n b_n \leq \max_n a_n / b_n$ for $a_n \geq 0, b_n > 0$.

In the following, we assume that the Lasso + OLS procedure is used in each nodewise selection. We first show that the symmetric property of the mirror statistics, or equivalently the screening property of the Lasso selection, is simultaneously satisfied in all p nodewise selections, with probability approaching 1 as $p \rightarrow \infty$, under the following assumptions.

Assumption 4 (a) *Regularity condition.* There exist positive constants c_0, c_1, c_2 such that

$$\lambda_{\min}(\Sigma) \geq c_0, \quad \max_{1 \leq j \leq p} \sigma_{jj} \leq c_1, \quad \max_{1 \leq j \leq p} \lambda_{jj} \leq c_2.$$

(b) *Sparsity condition.* There exists some $\xi \in [0, 1)$ such that

$$\max_{1 \leq j \leq p} |ne_j| = O(n_1^{\xi/2}).$$

(c) *The minimum-signal strength condition:*

$$\min\{|\lambda_{ij}| : \lambda_{ij} \neq 0, 1 \leq i < j \leq p\} \gtrsim \sqrt{\frac{\log p}{n_1^{1-\xi}}}.$$

Here n_1 is the sample size of the first half of data. Similar assumptions as Assumption 4(a) and 4(b) also appear in Liu (2013) and Meinshausen and Bühlmann (2006), respectively. Assumption 4(c) calibrates the minimum strength of the signal required for detection. It is commonly referred to as the ‘‘beta-min’’ condition in high-dimensional linear regressions (Dezeure et al., 2015). Under Assumption 4, we have the following proposition.

Proposition 4 *Under Assumption 4, if we apply the Lasso + OLS procedure to each nodewise regression with the regularization parameter properly chosen in the order of $O(\sqrt{\log p/n_1})$, then in the regime $n_1, p \rightarrow \infty$ and $\log p/n_1^{1-\xi/2} \rightarrow 0$, the symmetric assumption (Assumption 1) is simultaneously satisfied in all nodewise edge selection with probability approaching 1.*

The proof of Proposition 4 relies on Theorem 1 in Raskutti et al. (2010) and Theorem 7.2 in Bickel et al. (2009), and is postponed to the Appendix.

Under the symmetric assumption, we require some technical assumptions to asymptotically control the FDR of the estimated graph structure. The essential assumption is that for any $p \in \mathbb{N}_+$, $j \in [p]$, $t \in \mathbb{R}$, the set of Bernoulli random variables $\{\mathbb{1}(M_{ji} > t), i \in ne_j^c\}$ are only weakly dependent. For any subset $A \subseteq ne_j^c$, $k \in ne_j^c \setminus A$, and $t \in \mathbb{R}$, we define the following random variable to measure the conditional dependency,

$$\Delta_{p,j}^{k,A} = \left| \sum_{i \in ne_j^c} \mathbb{P} \left(M_{ji} > t \mid M_{jk} > t, \mathcal{F}_A \right) - \sum_{i \in ne_j^c} \mathbb{P} \left(M_{ji} > t \mid M_{jk} \leq t, \mathcal{F}_A \right) \right|, \quad (8)$$

in which \mathcal{F}_A denotes the sigma algebra generated by $\{\mathbb{1}(M_{ji} > t), i \in A\}$.

Assumption 5 (a) *There exist constants $C > 0$ and $\alpha \in (0, 1/2)$, such that for any $p \in \mathbb{N}_+$, $j \in [p]$, subset $A \subseteq ne_j^c$, $k \in ne_j^c \setminus A$, and $t \in \mathbb{R}$, we have $\Delta_{p,j}^{k,A} \leq C|ne_j^c|^\alpha$ almost surely.*

(b) $\lim_{p \rightarrow \infty} \min_{j \in [p]} |ne_j^c|^{1-2\alpha} / \log p = \infty$.

We remark that when all the indicators $\{\mathbb{1}(M_{ji} > t), i \in ne_j^c\}$ are independent, $\Delta_{p,j}^{k,A} \equiv 0$ for any subset $A \subseteq ne_j^c$ and $k \in ne_j^c \setminus A$. On the other hand, when all the indicators are perfectly correlated, i.e., $M_{j1} = \dots = M_{jp}$, we have $\Delta_{p,j}^{k,\emptyset} = |ne_j^c|$ for any $k \in ne_j^c$. We assume $\Delta_{p,j}^{k,A} \leq C|ne_j^c|^\alpha$ for some $\alpha \in (0, 1/2)$ almost surely to allow some weak dependency among $\{\mathbb{1}(M_{ji} > t), i \in ne_j^c\}$. Under Assumption 5, we have the following proposition. The proof is postponed to the Appendix.

Proposition 5 *Assume the symmetric assumption is satisfied in each nodewise edge selection. If we set the designated FDR control level for each nodewise edge selection to be $q/2$ and apply the Lasso + OLS procedure, then under Assumption 5, we can control the FDR of the estimated edge set \hat{E}_{OR} at the level q asymptotically as $p \rightarrow \infty$.*

We note that the nodewise selection procedure and the GFC approach proposed in Liu (2013) are effective in quite different scenarios. GFC tends to work well only if the underlying true graph is ultra-sparse, in the order of $o(\sqrt{n}/(\log p)^{3/2})$. The nodewise selection procedure is capable of handling the case when the graph is not too sparse, but can suffer from the ultra-sparsity. This can be seen by considering an extreme scenario where $|ne_j| = 1$ for some vertex X_j . Suppose with probability θ_j , $\max\{M_{ji} : i \in ne_j^c, M_{ji} > 0\}$ is strictly larger than $-\min\{M_{ji} : i \in ne_j^c, M_{ji} < 0\}$. Then the FDR of the nodewise selection of the vertex X_j is at least $0.5\theta_j$, since the FDP is at least 0.5. Therefore, if $\theta_j > q$, it is impossible to control FDR below $q/2$. We note that in the case where all $\{M_{ji} : i \in ne_j^c\}$ are independent and symmetric about 0, $\theta_j = 0.5$. A similar issue also exists in general knockoff-based approaches, which is pointed out in Remark 3.2 in Li and Maathuis (2019).

3.3 Deep neural network

In this section, we integrate the proposed data-splitting approaches into neural networks to achieve reproducible feature selection. We restrict ourselves here to fully-connected forward neural networks, although the procedure is easily applicable to more complex networks including convolutional neural networks and recurrent neural networks.

The recipe of our method is to first split the data into two halves, $(\mathbf{X}^{(1)}, \mathbf{y}^{(1)})$ and $(\mathbf{X}^{(2)}, \mathbf{y}^{(2)})$, and then train two neural networks with the same structure independently for each part of the data. Denote the number of units in each layer as m_h for $h \in [0 : k]$. The input layer is the 0-th layer with length $m_0 = p$, and the response layer is the k -th layer with length $m_k = 1$. For $h \in [k]$, let $\mathbf{H}^{(h)}$ be the vector of hidden units in layer h . In particular, we also write $\mathbf{H}^{(0)} = (X_1, \dots, X_p)$. Denote $\mathbf{W}^{(h)}$ as the $m_{h-1} \times m_h$ weight matrix between layer $h-1$ and layer h . Let ϕ_h be the activation function used between layer $h-1$ and layer h . Thus, we have $\mathbf{H}_\ell^{(h)} = \phi_h(\mathbf{H}^{(h-1)\top} \mathbf{W}_\ell^{(h)})$ for $\ell \in [m_h]$. Let the estimated weights be $\{\mathbf{W}^{(1,h)}\}_{h=1}^k$ and $\{\mathbf{W}^{(2,h)}\}_{h=1}^k$, where $\mathbf{W}^{(1,h)}$ and $\mathbf{W}^{(2,h)}$ are the $m_{h-1} \times m_h$ weight matrices between layer $h-1$ and layer h in the two trained neural networks, respectively. A cartoon illustration is given in Figure 3.

The main challenge of applying our FDR control approach to neural networks is to define a proper mirror statistic. A naive way is to calculate the mirror statistic only using the weights between the input layer and the first hidden layer. However, this proposal is problematic because the h -th layer's hidden units in the two

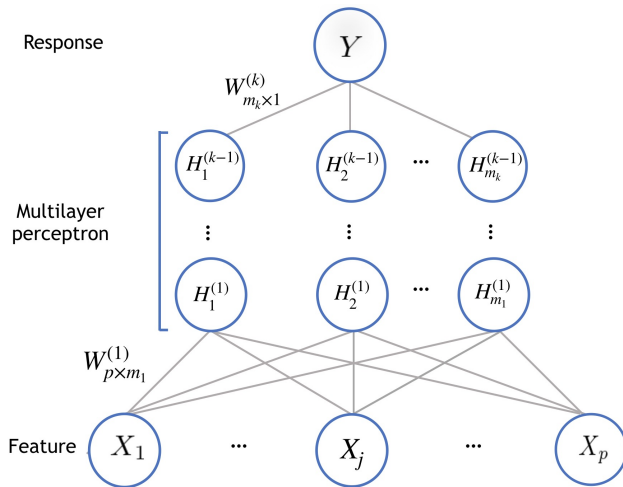


Figure 3: A demonstration of the fully-connected neural network.

neural networks, which are trained independently with different data and potentially different initialization, do not necessarily correspond to each other. Therefore, it is not sensible to directly contrast $\mathbf{W}_{j\ell}^{(1,1)}$ to $\mathbf{W}_{j\ell}^{(2,1)}$.

We discuss two alternatives to bypass the aforementioned non-identifiability problem of the hidden units. The first one is to use weight multiplication as in Lu et al. (2018). For each feature X_j , we define its “impact” coefficient $\hat{\beta}_j^{(1)}$ to be the j -th coordinate of the matrix product among all weights, that is, $\mathbf{W}^{(1,1)}\mathbf{W}^{(1,2)}\dots\mathbf{W}^{(1,k)}$. Similarly, we can define $\hat{\beta}_j^{(2)}$. This construction of the “impact” coefficient may only apply to fully-connected networks since in more complex networks such as convolutional neural networks, the weight tensor can be 3 or 4 dimensions, thus the multiplication between weight tensors are not well defined.

The second construction of the “impact” coefficient, which is able to handle more complex network structures, uses the influence function (Hechtlinger, 2016). It essentially calibrates the influence of feature X_j to the response variable y using gradient. Mathematically, the influence function, $\mathcal{I} = (\mathcal{I}_1, \dots, \mathcal{I}_p)$, is a vector of length p , with each coordinate defined to be $\mathcal{I}_j = \mathbb{E}[\partial f(X)/\partial X_j]$, where the expectation is taken with respect to the joint distribution of (y, X_1, \dots, X_p) . f represents the neural network model. Specifically, for fully-connected neural networks, the influence function can be explicitly written as:

$$\mathcal{I} = \mathbb{E} \left[\mathbf{W}^{(k)} \Phi^{(k)} \mathbf{W}^{(k-1)} \Phi^{(k-1)} \dots \mathbf{W}^{(1)} \Phi^{(1)} \right]. \quad (9)$$

$\Phi^{(h)}$ is a $m_h \times m_h$ diagonal matrix with ℓ -th element being the gradient of ϕ_h evaluated at the point $\mathbf{H}^{(h-1)\top} \mathbf{W}_{\cdot\ell}^{(h)}$ for $\ell \in [m_h]$. We proceed to approximate the influence function \mathcal{I} using the sample mean across training data, and its j -th coordinate will serve as the “impact” coefficient for feature X_j . We note that in most popular deep learning platforms, the gradient can be calculated using built-in functions, thus the computation is fairly user-friendly.

After obtaining the “impact” coefficient, the mirror statistic can be calculated following Equation (2). We note that the weight multiplication approach, which simply ignores all the activation functions between hidden layers, can be considered as a special case of the influence function approach. Although the two approaches seem to perform similarly in fully-connected forward networks based on our limited experiences, we believe that the influence function approach has more general applicability in real data examples.

4 Numerical Illustrations

4.1 Linear model

We consider the high-dimensional linear regression using Lasso. Throughout we fix the sample size $n = 500$ and the number of signals (sparsity) $s^* = 50$. We simulate the response variable \mathbf{y} from the linear model $\mathbf{y}_{n \times 1} = \mathbf{X}_{n \times p} \boldsymbol{\beta}_p + \boldsymbol{\epsilon}_{n \times 1}$, in which the noise $\boldsymbol{\epsilon}$ are sampled from $N(\mathbf{0}, I_n)$. We set $\beta_j = 0$ if $j > s^*$, and sample β_j from $N(0, \delta \sqrt{\log p/n})$ for $j \in [s^*]$. We consider the following two scenarios:

1. Vary the pairwise correlation among features. We independently sample each row of the design matrix $\mathbf{X}_{n \times p}$ from $N(\mathbf{0}_p, \Sigma)$, where $\Sigma_{jj} = 1$ and $\Sigma_{ij} = \rho$ for all $i \neq j$. We test out $\rho \in \{0.0, 0.2, 0.4, 0.6, 0.8\}$. Throughout this scenario, we fix the signal strength and set $\delta = 10$.
2. Vary the signal strength. We test out $\delta \in \{4, 8, 12, 16, 20\}$. Throughout this scenario, we sample independently each row of $\mathbf{X}_{n \times p}$ from $N(\mathbf{0}_p, \Sigma)$, where $\Sigma_{jj} = 1$ and $\Sigma_{ij} = 0.5$ for all $i \neq j$.

For each scenario, we also vary the total number of features $p \in \{500, 1000, 1500, 2000\}$.

We compare eight methods within three classes: (1) BHq and BYq; (2) the knockoff filter including the model-X knockoff filter (M-knockoff) (Candes et al., 2018), and the fixed-design knockoff filter (F-knockoff) based on data splitting, with the data recycling strategy proposed in Barber and Candès (2019); (3) DS and MDS. For BHq and BYq, we first randomly split the data into two halves. We then use one half of the data for signal screening using Lasso, and calculate the p-values for the selected features by running a OLS regression on the other half of the data. The corresponding multiple data-splitting versions (MBHq and MBYq) following Meinshausen et al. (2009), which combines the p-values obtained across multiple data splits, are also tested out using the R package *hdi*². We implement the model-X knockoff filter using the R package *knockoff*³. For the multiple data-splitting approaches MBHq, MBYq and MDS, we independently split the data 50 times. The designated FDR control level is set to be $q = 0.1$ in all simulation settings.

Figure 4 summarizes the results for the varying correlation scenario, in which $p \in \{500, 2000\}$ and $\rho \in \{0.0, 0.8\}$. More detailed results are given in Table 1 in the Appendix. The FDRs of all eight methods are reasonably under control across different simulation settings. The empirical performances show that MDS is promising. First, it significantly improves DS, in the sense that it simultaneously reduces the FDR and boosts the power. Second, from Table 1, we see that it has the highest power among all 8 methods when features are correlated ($\rho \geq 0.2$). When features are independent ($\rho = 0.0$), the power of MDS is second to the best, slightly lower than the power of the model-X knockoff filter. We note that $\rho = 0.0$ is considered to be the easiest setting for generating knockoff features as all the features are independent.

The following observations are also worthwhile to mention. First, when the correlation ρ is large, the model-X knockoff filter tends to be very conservative. From Table 1, we see that when $\rho \geq 0.4$, except for the relatively low-dimensional case $p = 500$, the model-X knockoff filter becomes powerless. On the other hand, the fixed-design knockoff filter is more robust to the dependency between features, and performs competitively across different simulation settings. Second, BYq is more conservative compared to BHq, which consistently yields a smaller FDR but also a lower power compared to BHq. We find that the p-value aggregation strategy proposed in Meinshausen et al. (2009) is effective. In most cases, MBHq and MBYq enjoy zero FDRs and competitive powers. The results for the varying signal strength scenario are summarized in Figure 5 and Table 2 in the Appendix, which provides similar evidence to demonstrate the effectiveness of the proposed data-splitting approaches.

4.2 Gaussian graphical model

We consider two types of graphs:

1. Banded graph. The precision matrix Λ is constructed such that $\lambda_{jj} = 1$, $\lambda_{ij} = \text{sign}(a) \cdot |a|^{|i-j|/c}$ if $0 < |i - j| \leq \rho$, and $\lambda_{ij} = 0$ if $|i - j| > \rho$. Following Li and Maathuis (2019), we set $c = 1.5$ throughout this simulation study. Other parameters including the sample size n , the dimension p , the signal strength (partial correlation) a , and the nodewise sparsity ρ will be specified case by case.
2. Blockwise diagonal graph. The precision matrix Λ is blockwise diagonal with equally sized squared blocks generated in the same fashion. We fix the block size to be 25×25 throughout this simulation study. In each block, all the diagonal elements are set to be 1, and the off-diagonal elements are independently sampled from some distribution u specified case by case.

The designated FDR control level is set to be $q = 0.2$. We note that for both graphs, the resulting precision matrix Λ is not necessarily positive definite. If $\lambda_{\min}(\Lambda) < 0$, we re-set $\Lambda \leftarrow \Lambda + (\lambda_{\min}(\Lambda) + 0.005)I_p$ following Liu (2013).

Three classes of competing methods are tested out: (1) DS and MDS; (2) BHq and BYq; (3) GFC-L and GFC-SL (two FDR control methods for Gaussian graphical model using Lasso or scaled Lasso proposed in

²<https://cran.r-project.org/web/packages/hdi/hdi.pdf>

³<https://cran.r-project.org/web/packages/knockoff/index.html>

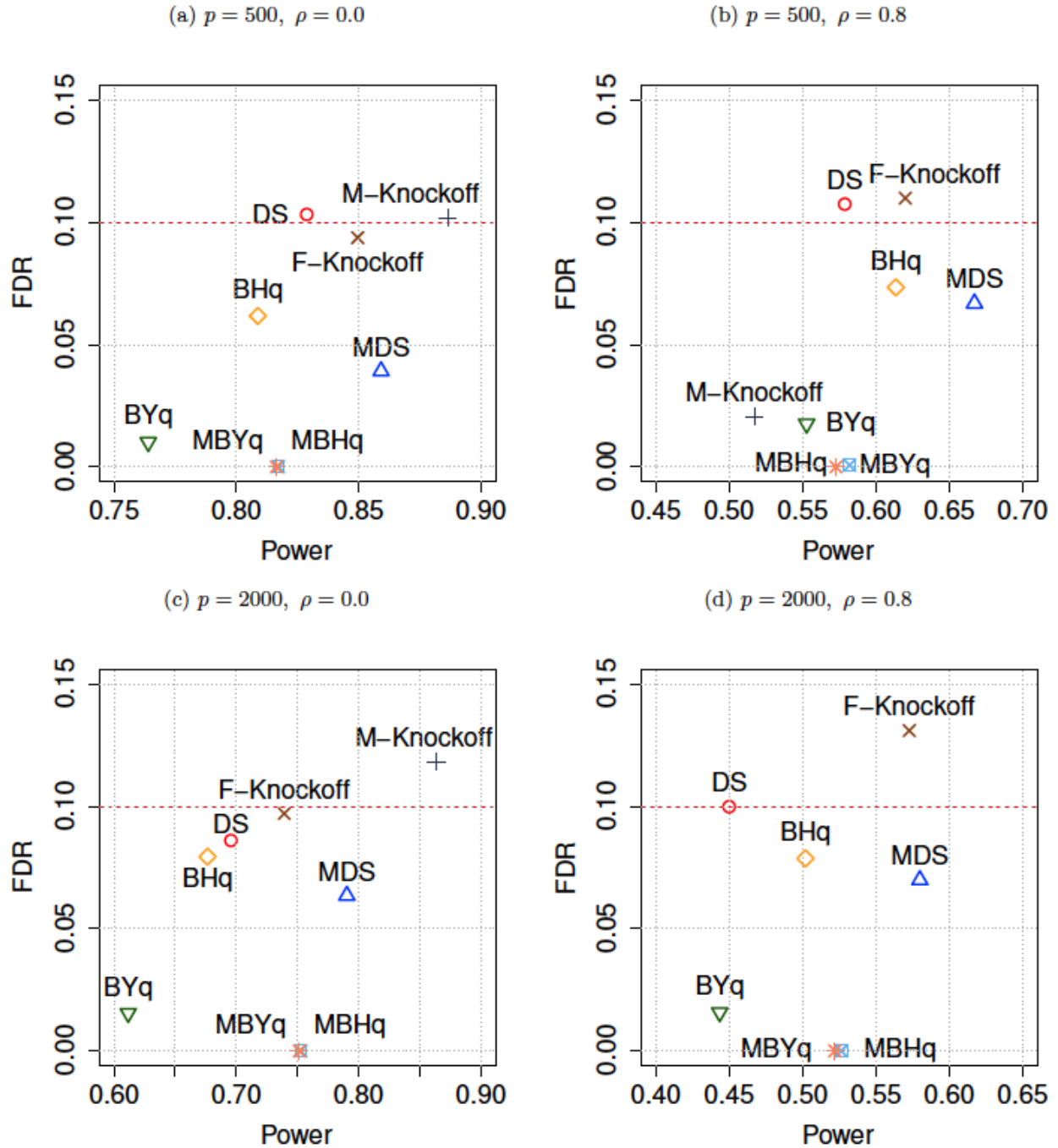


Figure 4: Empirical FDRs and powers on the linear model, where the design matrix has pairwise constant correlation ρ . The number of true features is 50 across all settings. The signal-to-noise ratio is $10 \times \sqrt{\log p/n}$. The designated FDR control level is $q = 0.1$ (the red dashed line). The eight methods are, the single data-splitting method (DS), the multiple data-splitting method (MDS), the model-X knockoff filter (M-Knockoff), the fixed-design knockoff filter with data recycling (F-Knockoff), the Benjamini-Hochberg method (BHq) and its multiple data-splitting version (MBHq), the Benjamini-Yekutieli method (BYq) and its multiple data-splitting version (MBYq). The reported results are the empirical means of 50 independent runs. In panel (d), the coordinates (Power, FDR) of the model-X knockoff filter (M-Knockoff) are (0.05, 0.00), which is out of range of the figure.

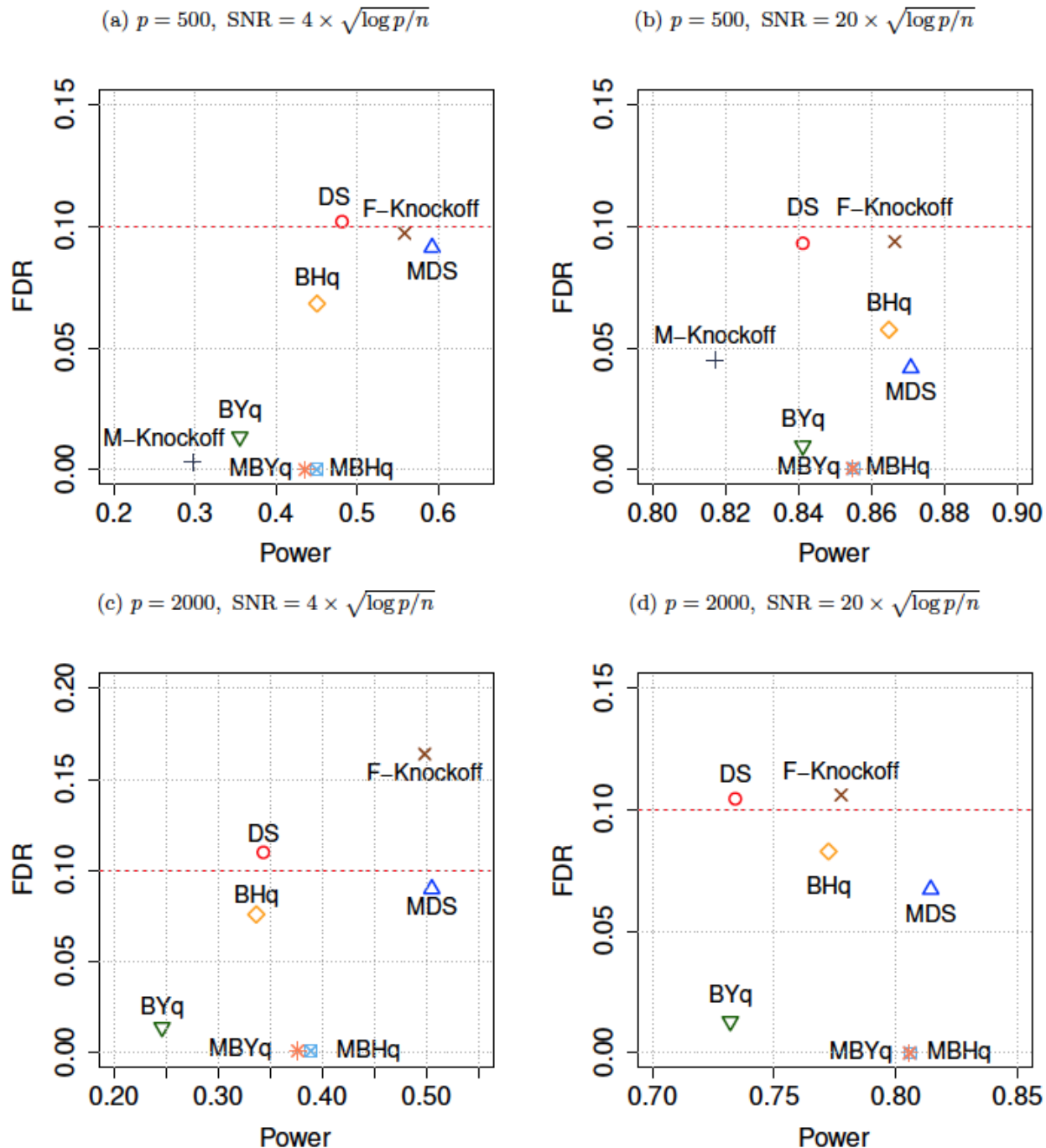


Figure 5: Empirical FDRs and powers on the linear model, where the design matrix follows a multivariate normal distribution with constant pairwise correlation 0.5. SNR represents the signal-to-noise ratio. The number of true features is 50 across all settings. The designated FDR control level is $q = 0.1$. The eight methods are, the single data-splitting method (DS), the multiple data-splitting method (MDS), the model-X knockoff filter (M-Knockoff), the fixed-design knockoff filter with data recycling (F-Knockoff), the Benjamini-Hochberg method (BHq) and its multiple-splitting version (MBHq), the Benjamini-Yekutieli method (BYq) and its multiple-splitting version (MBYq). The reported results are the empirical means of 50 independent runs. In panel (c) and panel (d), the coordinates (Power, FDR) of the model-X knockoff filter (M-Knockoff) are (0.04, 0.00) and (0.19, 0.00), respectively, which are out of range of the corresponding figures.

Liu (2013)). The p-values used in BHq and BYq are calculated based on the pairwise partial correlation test using the R package *ppcor* (Kim, 2015). We use the R package *SILGGM* (Zhang et al., 2018) to implement GFC-L and GFC-SL.

For the banded graph, we test out the following four settings:

- (a) Fix $p = 100$, $\rho = 8$, $a = -0.6$, and vary the sample size $n \in \{500, 1000, 1500, 2000, 2500\}$.
- (b) Fix $n = 1000$, $\rho = 8$, $a = -0.6$, and vary the dimension $p \in \{50, 100, 150, 200, 250\}$.
- (c) Fix $n = 1000$, $p = 100$, $a = -0.6$, and vary the nodewise sparsity $\rho \in \{4, 6, 8, 10, 12\}$.
- (d) Fix $n = 1000$, $p = 100$, $\rho = 8$, and vary the signal strength $a \in \{-0.5, -0.6, -0.7, -0.8, -0.9\}$.

For the blockwise diagonal graph, we fix $n = 500$, and test out three different scenarios, in which the sampling distribution u of the off-diagonal elements are set to be $\text{Unif}(-0.8, -0.4)$ (negative partial correlation), $\text{Unif}(0.4, 0.8)$ (positive partial correlation), and $\text{Unif}((-0.8, -0.4) \cup (0.4, 0.8))$ (balanced partial correlation), respectively. For MDS, we independently split the data 50 times and aggregate the selection results using Algorithm 2.

The results for the banded graphs are summarized in Figure 6. DS and MDS outperform the four competing methods across all simulation settings. In particular, MDS consistently yields a lower FDR and a higher power compared to DS. BYq has the lowest FDR, but appears to be too conservative as it also has the lowest power. FDRs of GFC-L, GFC-SL, and BHq are similar to each other, and are higher than FDRs of DS and MDS. In terms of power, GFC-L and GFC-SL perform similar, having a slightly higher power than BHq. Panel (d) in Figure 6 is interesting, since the powers of BHq and BYq have an opposite trend compared to the other methods. One possible reason is that when we decrease the signal strength, or equivalently increase a from -0.9 to -0.5 , the pairwise correlations decrease from 0.54 to 0.20 so that the independent p-value assumption becomes better justified. Therefore, we see a power increase for BHq and BYq.

The results for the blockwise diagonal graphs are summarized in Figure 7. In the settings with balanced signals and negative signals, MDS outperforms all the other competing methods. In particular, in the setting with negative signals, DS and MDS are the only two effective methods with reasonable powers. In the setting with positive partial correlation, BHq and BYq are the two leading methods. In this scenario, DS and MDS perform reasonably well only in the low-dimensional setting.

4.3 Deep neural network

We consider the single-index model $y = f(\mathbf{x}^\top \boldsymbol{\beta}) + \epsilon$, in which $f(t)$ is some unknown link function, and ϵ is the noise. In this simulation study, we test out three different cases detailed below.

1. Power function. We set $f_1(t) = t^3/2$.
2. Exponential function. We set $f_2(t) = \exp(t/10)$.
3. Sigmoid function. We set $f_3(t) = 1/(1 + \exp(-t))$.

For the power function and the exponential function, we set the number of signals (sparsity) $s^* = 30$, and sample the randomly located nonzero β_j from $N(0, 20 \times \sqrt{\log p/n})$. For the sigmoid function, we set the number of signals (sparsity) $s^* = 50$, and sample the randomly located nonzero β_j from $\text{Unif}(0.5, 1)$. For the power function, we assume ϵ follows $N(0, 1)$. For the exponential function and the sigmoid function, we decrease the noise level by assuming ϵ follows $N(0, 0.1^2)$. Throughout we fix the sample size $n = 1000$, and vary $p \in \{500, 1000, 1500, 2000, 3000\}$ for all three cases. The designated FDR control level is fixed to be $q = 0.1$. For the design matrix \mathbf{X} , in which each row is independently simulated from $N(0, \Sigma)$, we test out two cases: (1) we assume the precision matrix $\Sigma_{ij}^{-1} = \rho^{|i-j|}$; (2) we assume the covariance matrix $\Sigma_{ij} = \rho^{|i-j|}$. ρ is fixed to be 0.5 across all settings.

We compare the proposed data-splitting methods using the influence function or the weight multiplication, and the DeepPINK method proposed in Lu et al. (2018). For DS and MDS, we build a four-layer fully-connected neural network. The input layer is of size p , the output layer is of size 1 , and the two hidden layers in the middle are of size $20 \times \log(p)$ and $10 \times \log(p)$, respectively. We choose sigmoid as the activation function between the first three layers, and add a ℓ_1 regularization term of the order $O(\sqrt{\log p/n})$ for the two hidden layers. For DeepPINK, we test out two architectures of the neural network. DeepPINK-I has the

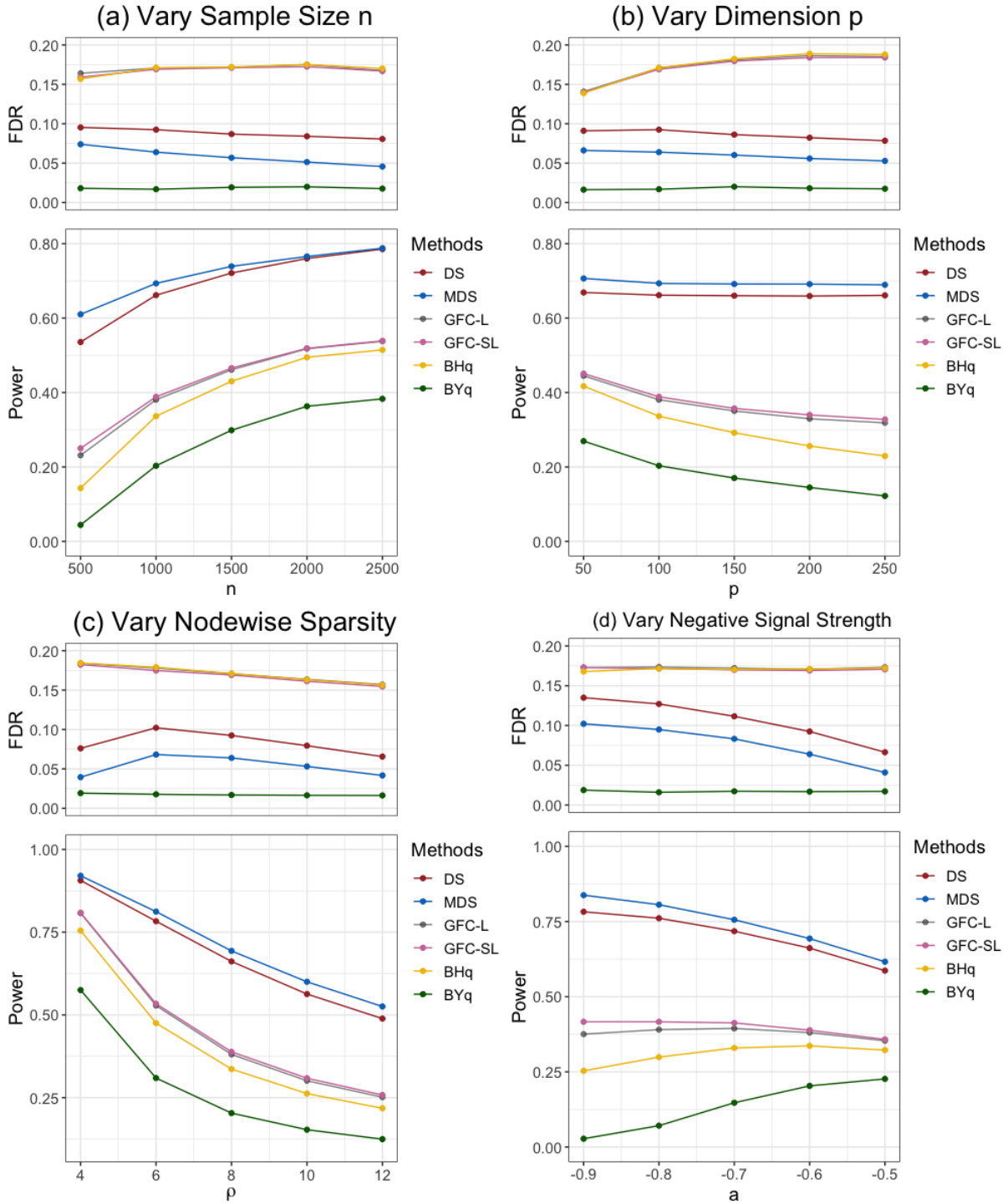


Figure 6: Empirical FDRs and powers on the banded graphs of the six methods, the single data-splitting method (DS), the multiple data-splitting method (MDS), the GFC methods with Lasso (GFC-L) and scaled Lasso (GFC-SL) proposed in Liu (2013), the Benjamini-Hochberg method (BHq), and the Benjamini-Yekutieli method (BYq). The designated FDR control level is $q = 0.2$ in all settings. The reported results are the empirical means of 50 independent runs.

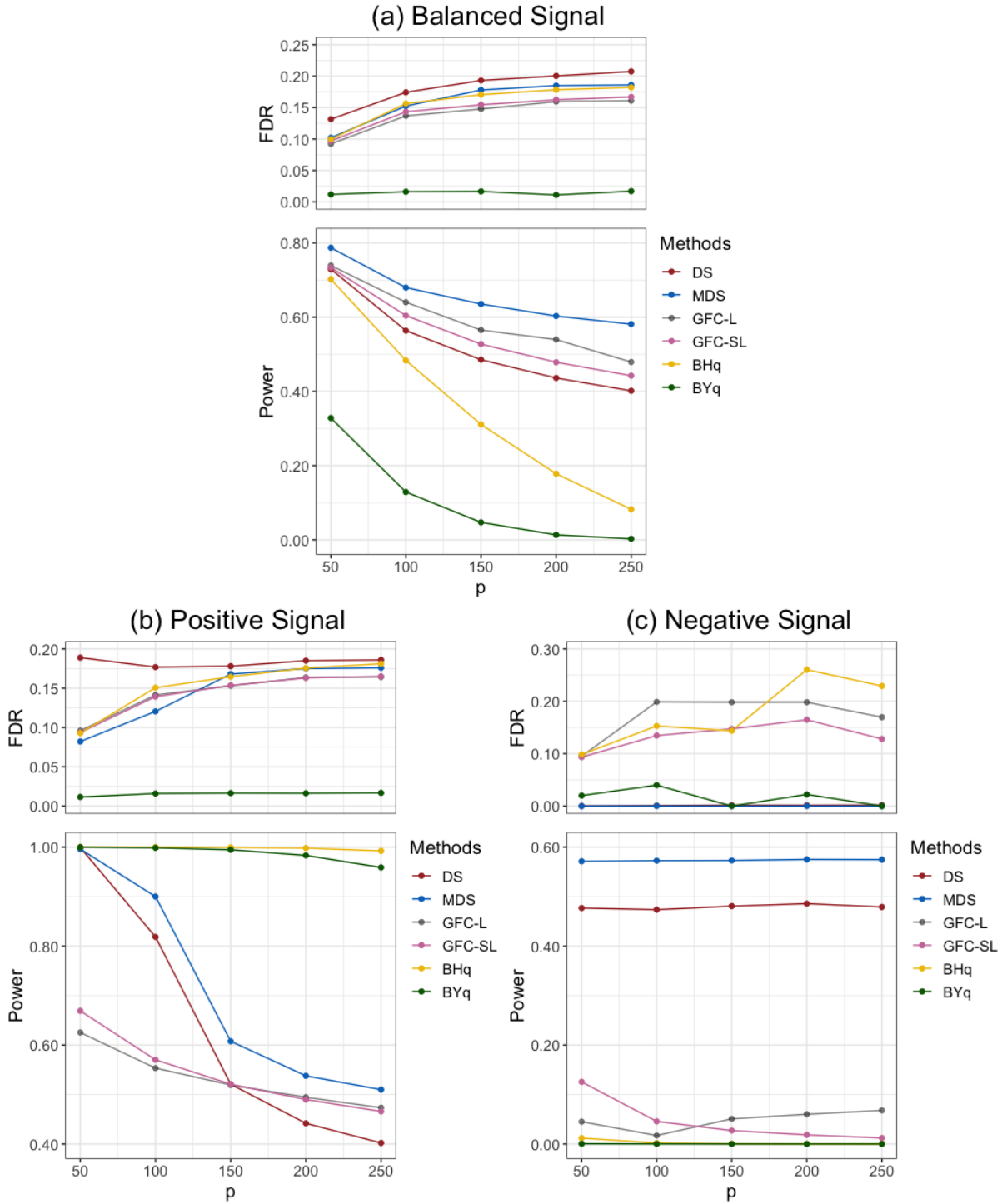


Figure 7: Empirical FDRs and powers on the blockwise diagonal graphs with different partial correlation ranges. The six methods are, the single data-splitting method (DS), the multiple data-splitting method (MDS), the GFC methods with Lasso (GFC-L) and scaled Lasso (GFC-SL) proposed in Liu (2013), the Benjamini-Hochberg method (BHq), and the Benjamini-Yekutieli method (BYq). The designated FDR control level is $q = 0.2$ in all settings. The reported results are the empirical means of 50 independent runs.

same architecture as described in Lu et al. (2018) (see the caption of Figure 1), whereas DeepPINK-II has the same architecture as DS and MDS. We set the batch size to be 128 and set the initializing learning rate to be 0.001. We use the Adam algorithm (Kingma and Ba, 2014) to train the neural network with respect to the mean squared error loss for a total of 500 epochs. For MDS, we randomly split the data 50 times, and aggregate the selection results based on Algorithm 2. For the DeepPINK method, we thank the authors for kindly providing their code through personal communication.

The results for $p = 2000$ are summarized in Figure 8, and more detailed results for different p are given in Table 3 and Table 4 in the Appendix. Compared to the DeepPINK method, DS and MDS consistently yield smaller FDR and significantly higher power. For DS and MDS, the influence function approach and the weight multiplication approach yield similar results. Compared with DS, MDS always has a lower FDR value, but also slightly lower power in cases $f_2(t)$ and $f_3(t)$.

4.4 Real data application: HIV drug resistance

We apply the proposed approaches to detect mutations in the Human Immunodeficiency Virus Type 1 (HIV-1) that are associated with drug resistance. The data set, which has also been analyzed in Rhee et al. (2006), Barber and Candès (2015), and Lu et al. (2018), contains resistance measurements of 7 drugs for protease inhibitors (PIs), 6 drugs for nucleoside reverse-transcriptase inhibitors (NRTIs), and 3 drugs for nonnucleoside reverse transcriptase inhibitors (NNRTIs). We focus on the first two classes of inhibitors, PI and NRTI, as in Lu et al. (2018).

The response variable \mathbf{y} calibrates the log-fold-increase of lab-tested drug resistance. The design matrix \mathbf{X} is binary, in which the j th column indicates the presence or absence of the j th mutation. The task is to select relevant mutations for each inhibitor against different drugs. The data is preprocessed as follows. First, we remove the patients with missing drug resistance information. Second, we only focus on those mutations that appear at least three times across all the patients. The sample size n and the number of mutations p vary from drug to drug, but are all in hundreds with n/p ranging from 1.5 to 4 (see Figures 9 and 10). We assume an additive linear model between the response variable and the features with no interactions.

Five methods are compared, including DeepPINK with model-X knockoffs (Lu et al., 2018), the fixed-design knockoff filter based on a Gaussian linear model (Barber and Candès, 2015), BHq, DS, and MDS. For DeepPINK, knockoff, and BHq, we report the selection results obtained in Lu et al. (2018). The designated FDR control level is $q = 0.2$ throughout. The results are evaluated based on the selected mutations with existing treatment-selected mutation (TSM) panels (Rhee et al., 2005), as discussed in Barber and Candès (2015).

Numbers of discovered mutations for PI within each drug class, including both true and false positives, are summarized in Figure 9. We see that MDS performs the best for 4 out of 7 PI drugs, including ATV, LPV, NFV, and SQV. For the remaining drugs, APV, IDV and RTV, MDS is comparable to DeepPINK, and both are superior to the fixed-design knockoff filter and BHq. Similarly, Figure 10 shows the numbers of the identified mutations for the NRTI drugs. Among the 6 NRTI drugs, MDS performs the best in 5, including ABC, AZT, D4T, DDI, and X3TC. For TDF, MDS is comparable to DeepPINK, and both are much better than BHq and the fixed-design knockoff filter. In particular, the fixed-design knockoff filter has no power and does not select any mutation for DDI, TDF, and X3TC.

5 Concluding Remarks

We have described a general framework for the FDR control in the task of high-dimensional feature selection. The proposed data-splitting approaches (DS and MDS) allow us to asymptotically control FDR in canonical statistical models including the linear model and the Gaussian graphical model. We have also empirically demonstrated its applications to more complex models such as deep neural networks. The multiple data-splitting approach (MDS) proposed here is of particular interest, which helps stabilize the selection result and remedy the potential power loss. Both DS and MDS are conceptually simple and easy to implement based upon existing softwares for high-dimensional feature selection methods.

We conclude by pointing out several directions for future work. First, for the linear model, an interesting extension of the Lasso + OLS procedure is to consider features with a group structure. A natural strategy is to substitute Lasso with group Lasso. However, unlike Lasso, group Lasso can potentially select more than n features (n is the sample size), thus the companion OLS step, which guarantees the symmetric assumption, may not be easily applied. Second, we would like to apply the proposed framework, equipped with the

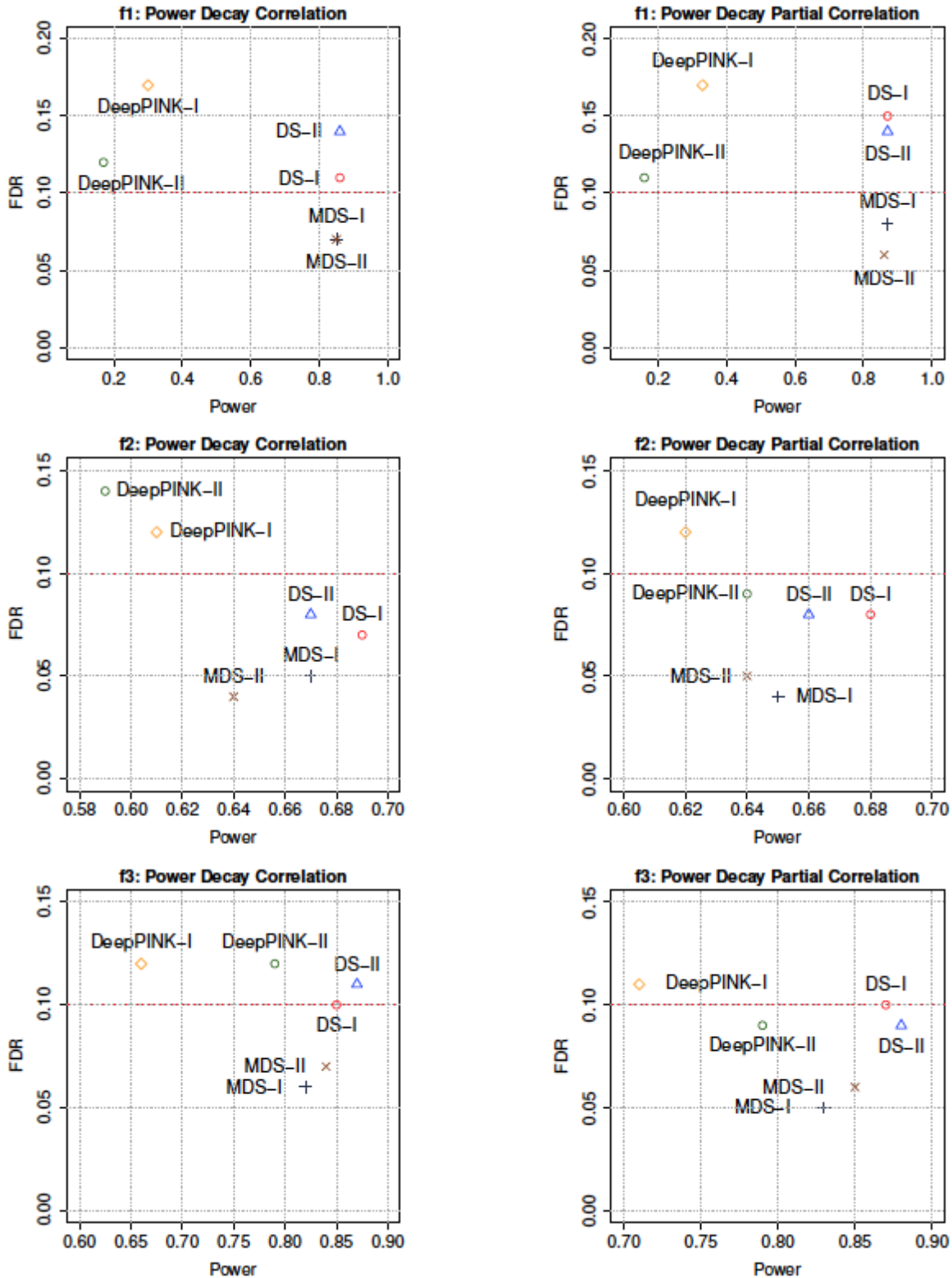


Figure 8: Empirical FDRs and powers on the single-index models for $p = 2000$. The design matrix follows multivariate normal distribution with pairwise power decay correlation (the left column) or pairwise power decay partial correlation (the right column). The six methods are, the single data-splitting method using the influence function (DS-I) and its multiple data-splitting version (MDS-I), the single data-splitting method using the weight multiplication (DS-II) and its multiple data-splitting version (MDS-II), and the DeepPINK method with two different network architectures (see the text for details). The designated FDR control level is $q = 0.1$ (the red dashed line) in all settings. The reported results are the empirical means of 20 independent runs.

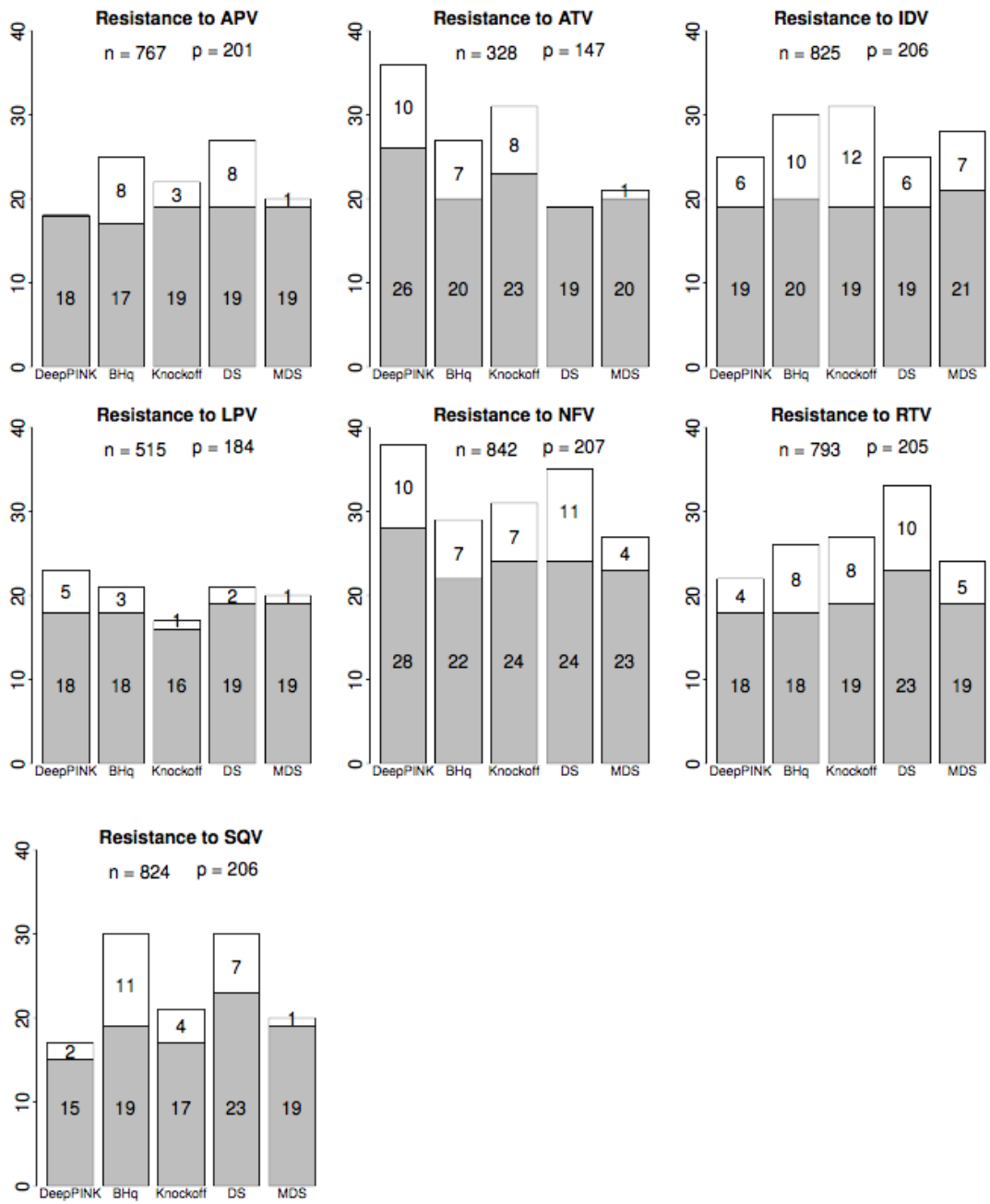


Figure 9: Numbers of discovered mutations corresponding to the 7 PI drugs. The grey bar represents the number of true positives, while the white bar represents the number of false positives. The designated FDR control level is $q = 0.2$.

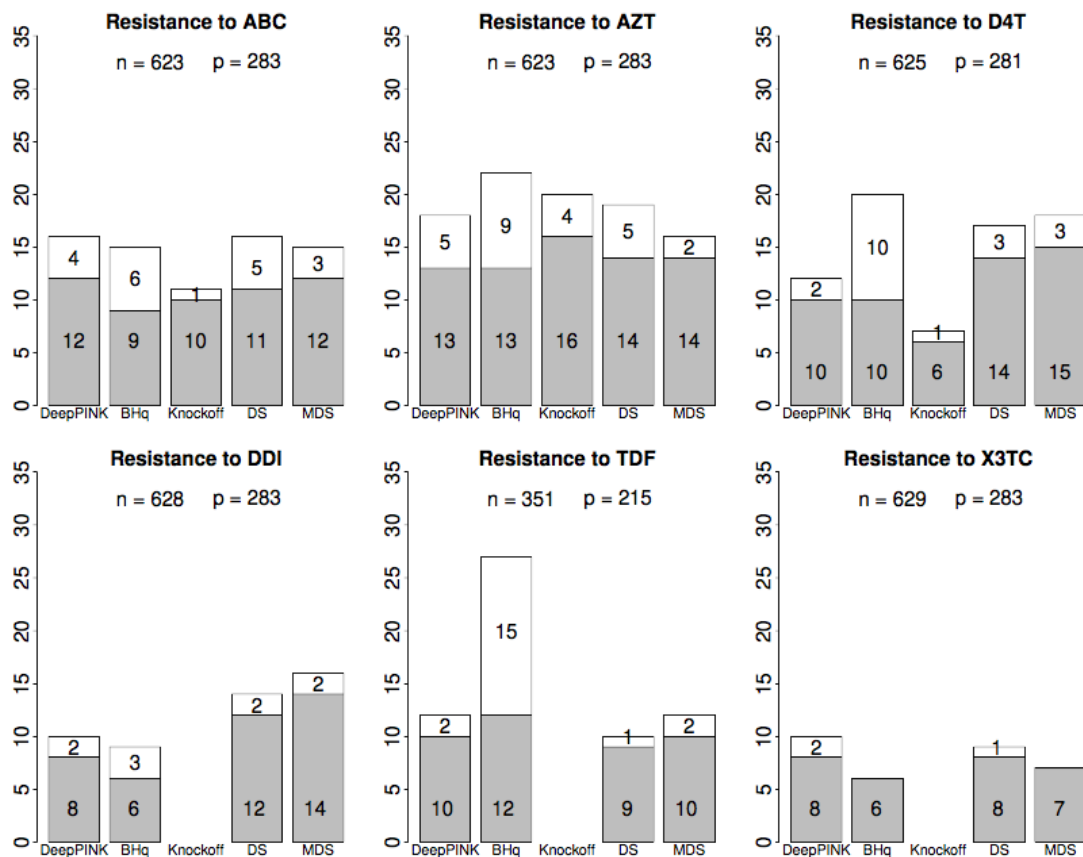


Figure 10: Numbers of discovered mutations corresponding to the 6 NRTI drugs. The grey bar represents the number of true positives, while the white bar represents the number of false positives. The designated FDR control level is $q = 0.2$.

influence function, to convolutional neural networks and recurrent neural networks, in order to handle more complex data such as images and natural languages. Third, we are interested in investigating the multiple testing problem of sparse high-dimensional covariance matrices, which are commonly estimated using some thresholding estimator. Our proposed framework is applicable as long as the estimator to the zero covariance element is symmetric about 0. Last but not the least, extensions of the DS and MDS frameworks to data containing dependent observations or having hierarchical structures can be of immediate interest.

6 Appendix

6.1 Proofs

6.1.1 Proof of Proposition 1

For the ease of presentation, we introduce the following notations. For $t \in \mathbb{R}$, denote

$$\begin{aligned}\widehat{G}_p^0(t) &= \frac{1}{p_0} \sum_{j \in S_0} \mathbb{1}(M_j > t), & \widehat{V}_p^0(t) &= \frac{1}{p_0} \sum_{j \in S_0} \mathbb{1}(M_j < -t), \\ \widehat{G}_p^1(t) &= \frac{1}{p_1} \sum_{j \in S^*} \mathbb{1}(M_j > t), & G_p^0(t) &= \frac{1}{p_0} \sum_{j \in S_0} \mathbb{P}(M_j > t).\end{aligned}\tag{10}$$

Let $r_p = p_1/p_0$. In addition, denote

$$\text{FDP}_p(t) = \frac{\widehat{G}_p^0(t)}{\widehat{G}_p^0(t) + r_p \widehat{G}_p^1(t)}, \quad \text{FDP}_p^\dagger(t) = \frac{\widehat{V}_p^0(t)}{\widehat{G}_p^0(t) + r_p \widehat{G}_p^1(t)}, \quad \overline{\text{FDP}}_p(t) = \frac{G_p^0(t)}{G_p^0(t) + r_p \widehat{G}_p^1(t)}.\tag{11}$$

Lemma 2 *Under Assumption 2, if $p_0 \rightarrow \infty$ as $p \rightarrow \infty$, we have in probability,*

$$\sup_{t \in \mathbb{R}} \left| \widehat{G}_p^0(t) - G_p^0(t) \right| \rightarrow 0, \quad \sup_{t \in \mathbb{R}} \left| \widehat{V}_p^0(t) - G_p^0(t) \right| \rightarrow 0.\tag{12}$$

Proof of Lemma 2. For any $\epsilon \in (0, 1)$, denote $-\infty = \alpha_0^p < \alpha_1^p < \dots < \alpha_{N_\epsilon}^p = \infty$ in which $N_\epsilon = \lceil 2/\epsilon \rceil$, such that $G_p^0(\alpha_{k-1}^p) - G_p^0(\alpha_k^p) \leq \epsilon/2$ for $k \in [N_\epsilon]$. Such a sequence $\{\alpha_k^p\}$ exists because by Assumption 2, all the mirror statistics M_j 's are continuous random variables so that $G_p^0(t)$ is a continuous function with respect to $t \in \mathbb{R}$. We have

$$\begin{aligned}\mathbb{P} \left(\sup_{t \in \mathbb{R}} \widehat{G}_p^0(t) - G_p^0(t) > \epsilon \right) &\leq \mathbb{P} \left(\bigcup_{k=1}^{N_\epsilon} \sup_{t \in [\alpha_{k-1}^p, \alpha_k^p]} \widehat{G}_p^0(t) - G_p^0(t) > \epsilon \right) \\ &\leq \sum_{k=1}^{N_\epsilon} \mathbb{P} \left(\sup_{t \in [\alpha_{k-1}^p, \alpha_k^p]} \widehat{G}_p^0(t) - G_p^0(t) > \epsilon \right).\end{aligned}\tag{13}$$

We note that both $\widehat{G}_p^0(t)$ and $G_p^0(t)$ are monotonic decreasing function. Therefore, for any $k \in [N_\epsilon]$, we have

$$\sup_{t \in [\alpha_{k-1}^p, \alpha_k^p]} \widehat{G}_p^0(t) - G_p^0(t) \leq \widehat{G}_p^0(\alpha_{k-1}^p) - G_p^0(\alpha_k^p) \leq \widehat{G}_p^0(\alpha_{k-1}^p) - G_p^0(\alpha_{k-1}^p) + \epsilon/2.\tag{14}$$

Based on Equation (13), Assumption 2, and the Chebyshev's inequality, it follows that

$$\mathbb{P} \left(\sup_{t \in \mathbb{R}} \widehat{G}_p^0(t) - G_p^0(t) > \epsilon \right) \leq \sum_{k=1}^{N_\epsilon} \mathbb{P} \left(\widehat{G}_p^0(\alpha_{k-1}^p) - G_p^0(\alpha_{k-1}^p) > \frac{\epsilon}{2} \right) \leq \frac{4CN_\epsilon}{p_0^{2-\alpha_\epsilon} \epsilon^2} \rightarrow 0, \quad \text{as } p \rightarrow \infty.\tag{15}$$

Similarly, we can show that

$$\mathbb{P} \left(\inf_{t \in \mathbb{R}} \widehat{G}_p^0(t) - G_p^0(t) < -\epsilon \right) \leq \sum_{k=1}^{N_\epsilon} \mathbb{P} \left(\widehat{G}_p^0(\alpha_k^p) - G_p^0(\alpha_k^p) < -\frac{\epsilon}{2} \right) \leq \frac{4CN_\epsilon}{p_0^{2-\alpha_\epsilon} \epsilon^2} \rightarrow 0, \quad \text{as } p \rightarrow \infty.\tag{16}$$

This concludes the proof that $\sup_{t \in \mathbb{R}} \left| \widehat{G}_p^0(t) - G_p^0(t) \right| \rightarrow 0$ in probability. The convergence of $\sup_{t \in \mathbb{R}} \left| \widehat{V}_p^0(t) - G_p^0(t) \right|$ can be shown similarly using the symmetric assumption of the mirror statistics M_j for $j \in S_0$.

Proof of Proposition 1. Notice that

$$\begin{aligned}
\limsup_{p \rightarrow \infty} \text{FDR} &\leq \limsup_{p \rightarrow \infty} \mathbb{E} [\text{FDP}_p(\tau_q)] \leq \limsup_{p \rightarrow \infty} \mathbb{E} \left| \text{FDP}_p(\tau_q) - \overline{\text{FDP}}_p(\tau_q) \right| \\
&\quad + \limsup_{p \rightarrow \infty} \mathbb{E} \left| \text{FDP}_p^\dagger(\tau_q) - \overline{\text{FDP}}_p(\tau_q) \right| + \limsup_{p \rightarrow \infty} \mathbb{E} \left[\text{FDP}_p^\dagger(\tau_q) \right] \\
&\leq \limsup_{p \rightarrow \infty} \mathbb{E} \left[\sup_{t > 0} \left| \text{FDP}_p(t) - \overline{\text{FDP}}_p(t) \right| \right] + \limsup_{p \rightarrow \infty} \mathbb{E} \left[\sup_{t > 0} \left| \text{FDP}_p^\dagger(t) - \overline{\text{FDP}}_p(t) \right| \right] \\
&\quad + \limsup_{p \rightarrow \infty} \mathbb{E} \left[\text{FDP}_p^\dagger(\tau_q) \right].
\end{aligned} \tag{17}$$

The first two terms are 0 based on Lemma 2 and the dominated convergence theorem. For the last term, we have $\text{FDP}_p^\dagger(\tau_q) \leq q$ almost surely based on the definition of τ_q . This concludes the proof of Proposition 1.

6.1.2 Proof of Proposition 2

Lemma 3 For any FDR level $q \in (0, 1)$, let ℓ be the largest value in $[p]$ such that $I_{(1)} + \dots + I_{(\ell)} \leq q$, where $0 \leq I_{(1)} \leq I_{(2)} \leq \dots \leq I_{(p)}$ are the order statistics of the population inclusion rates. Let $p_0 = |S_0|$, $p_1 = |S^*|$, and $p = p_0 + p_1$. Under Assumption 3(a) and 3(c), when $p_0 \rightarrow \infty$, we have

$$\liminf_{p \rightarrow \infty} \frac{\ell}{p_0} \geq 1. \tag{18}$$

Proof of Lemma 3. Because ℓ is the largest index in $[p]$ such that $I_{(1)} + \dots + I_{(\ell)} \leq q$, we have $I_{(1)} + \dots + I_{(\ell+1)} > q$. Therefore, $I_{(\ell+1)} > q/(\ell+1)$. By Assumption 3(c), for any $\epsilon > 0$, there exists \tilde{p} , such that when $p \geq \tilde{p}$, we have $\sum_{j \in S_0} I_j \leq q + \epsilon$. By Assumption 3(a), we have $I_j \leq (q + \epsilon)/p_0$ for any $j \in S_0$. We next consider the following two cases. (1) If $q/(\ell+1) \geq (q + \epsilon)/p_0$, we have $I_j < I_{(\ell+1)}$ for any $j \in S_0$. Therefore $\ell \geq p_0$. (2) If $q/(\ell+1) < (q + \epsilon)/p_0$, we have

$$\frac{\ell}{p_0} > \frac{q}{q + \epsilon} - \frac{1}{p_0}. \tag{19}$$

Because ϵ can be arbitrarily small and $p_0 \rightarrow \infty$, we conclude the proof.

Proof of Proposition 2. By Assumption 3(c), for any $\epsilon > 0$, there exists \tilde{p}' , such that when $p \geq \tilde{p}'$, we have $\sum_{j \in S_0} I_j \leq q + \epsilon$. By Assumption 3(a), we have $I_j \leq (q + \epsilon)/p_0$ for any $j \in S_0$. By Assumption 3(b), with the same ϵ as before and $\alpha = (q + \epsilon)/p_0$, there exists \tilde{p}'' , such that when $p \geq \tilde{p}''$, we have

$$\frac{1}{p_1} \# \left\{ j : j \in S^*, I_j \leq \frac{q + \epsilon}{p_0} \right\} \leq q + 2\epsilon. \tag{20}$$

By Lemma 3, with the same ϵ as before, there exists \tilde{p}''' , such that when $p \geq \tilde{p}'''$, we have $\ell/p_0 \geq 1 - \epsilon$. In the following, we assume $p \geq \max\{\tilde{p}', \tilde{p}'', \tilde{p}'''\}$. We next consider the following two cases. (1) If $I_{(\ell)} > (q + \epsilon)/p_0$, then $I_{(\ell)} > I_j$ for any $j \in S_0$. This implies that none of the null features will be selected, thus the FDR is simply 0. (2) If $I_{(\ell)} \leq (q + \epsilon)/p_0$, we have

$$\begin{aligned}
\frac{\sum_{j \in S_0} \mathbb{1}(I_j > I_{(\ell)})}{\sum_{j=1}^p \mathbb{1}(I_j > I_{(\ell)}) \vee 1} &= 1 - \frac{\sum_{j \in S^*} \mathbb{1}(I_j > I_{(\ell)})}{\sum_{j=1}^p \mathbb{1}(I_j > I_{(\ell)}) \vee 1} \leq 1 - \frac{\sum_{j \in S^*} \mathbb{1}(I_j > (q + \epsilon)/p_0)}{p - \ell} \\
&\leq 1 - \frac{p_1 - (q + 2\epsilon)p_1}{p - \ell} \leq 1 - \frac{p_1 - (q + 2\epsilon)p_1}{p - p_0(1 - \epsilon)} \\
&= q + \frac{(1 - q + p_1/p_0)\epsilon}{p_1/p_0 + \epsilon}.
\end{aligned} \tag{21}$$

Because ϵ can be arbitrarily small and $\liminf_{p \rightarrow \infty} p_1/p_0 > 0$, we conclude the proof.

6.1.3 Proof of Proposition 3

Suppose $p_j \leq p'_j$. Let $Z_j = \bar{\mathbf{X}}_j^{(1)} - \bar{\mathbf{X}}_j^{(2)}$ be the difference of the two sample means, which follows $N(0, 4\sigma^2/n)$ regardless of the data split. Z_j is also independent to $\bar{\mathbf{X}}_j = (\bar{\mathbf{X}}_j^{(1)} + \bar{\mathbf{X}}_j^{(2)})/2$ because of the normality. The mirror statistic is thus $M_j = |2\bar{\mathbf{X}}_j| - |Z_j|$. It is sufficient for us to prove that $\mathbb{E}[\mathbb{1}(j \in \hat{S})/(|\hat{S}| \vee 1) | |\bar{\mathbf{X}}_j|]$ is a monotone increasing function of $|\bar{\mathbf{X}}_j|$. By conditioning on Z_j , we have

$$\mathbb{E} \left[\frac{\mathbb{1}(j \in \hat{S})}{|\hat{S}| \vee 1} \middle| \bar{\mathbf{X}}_j \right] - \mathbb{E} \left[\frac{\mathbb{1}(j \in \hat{S}')}{|\hat{S}'| \vee 1} \middle| \bar{\mathbf{X}}'_j \right] = \mathbb{E} \left(\mathbb{E} \left[\frac{\mathbb{1}(j \in \hat{S})}{|\hat{S}| \vee 1} \middle| \bar{\mathbf{X}}_j, Z_j \right] - \mathbb{E} \left[\frac{\mathbb{1}(j \in \hat{S}')}{|\hat{S}'| \vee 1} \middle| \bar{\mathbf{X}}'_j, Z_j \right] \right). \quad (22)$$

By conditioning on $\bar{\mathbf{X}}_j, Z_j$ and $\bar{\mathbf{X}}'_j, Z_j$, we have $M_j \geq M'_j$. For any realization of the rest of data X_{ik} for $i \in [n]$ and $k \neq j$, which is independent to $\bar{\mathbf{X}}_j, Z_j$ and $\bar{\mathbf{X}}'_j, Z_j$, we have $\mathbb{1}(j \in \hat{S})/(|\hat{S}| \vee 1) \geq \mathbb{1}(j \in \hat{S}')/(|\hat{S}'| \vee 1)$. This can be argued by considering the three cases including $\tau_q \leq M'_j$, $M'_j \leq \tau_q < M_j$, and $\tau_q \geq M_j$, where τ_q is the cutoff of mirror statistics defined in Equation (3). In the first case, we have $\mathbb{1}(j \in \hat{S})/(|\hat{S}| \vee 1) = \mathbb{1}(j \in \hat{S}')/(|\hat{S}'| \vee 1) = 1/(|\hat{S}| \vee 1)$, while in the third case, we have $\mathbb{1}(j \in \hat{S})/|\hat{S}| = \mathbb{1}(j \in \hat{S}')/|\hat{S}'| = 0$. In the second case, since $\mathbb{1}(j \in \hat{S}') = 0$, we have $\mathbb{1}(j \in \hat{S})/(|\hat{S}| \vee 1) \geq \mathbb{1}(j \in \hat{S}')/(|\hat{S}'| \vee 1)$.

6.1.4 Proof of Proposition 4

Denote $s = \max_{1 \leq j \leq p} |ne_j|$. We first show that the restricted eigenvalue condition in Bickel et al. (2009), page 1710, holds with probability approaching 1 in the regime $\log p/n_1^{1-\xi/2} \rightarrow 0$. For the j th nodewise egde selection, for any $J_0 \subseteq [1 : p] \setminus \{j\}$ with $|J_0| \leq s$, and any $\mathbf{v} \neq \mathbf{0}$ satisfying $\|\mathbf{v}_{J_0^c}\|_1 \leq \|\mathbf{v}_{J_0}\|_1$, we have $\|\mathbf{v}\|_1 \leq 2\|\mathbf{v}_{J_0}\|_1 \leq 2\sqrt{s}\|\mathbf{v}\|_2$. By Theorem 1 in Raskutti et al. (2010) and Cauchy interlacing theorem, with high probability, we have:

$$\frac{\|\mathbf{X}_{-j}^{(1)}\mathbf{v}\|_2}{\sqrt{n_1}} \geq \left(\frac{1}{4} \lambda_{\min}(\Sigma) - 18 \max_{1 \leq j \leq p} \sigma_{jj} \sqrt{\frac{s \log p}{n_1}} \right) \|\mathbf{v}\|_2. \quad (23)$$

Under Assumption 4, we have

$$\max_{1 \leq j \leq p} \sigma_{jj} \sqrt{\frac{s \log p}{n_1}} \rightarrow 0, \quad (24)$$

thus $\kappa(s, 1) \gtrsim \sqrt{c_0}$ with probability approaching 1. Now we apply the high probability ℓ_1 -bound (Equation (7.4) in Bickel et al. (2009)), which is asymptotically no larger than $\sqrt{\log p/n_1^{1-\xi}}$. Therefore by Assumption 4(c), we conclude that the screening property, thus the symmetric assumption, will hold with probability approaching 1 in the regime $\log p/n_1^{1-\xi/2} \rightarrow 0$.

6.1.5 Proof of Proposition 5

For the ease of presentation, we introduce the following notations. For $j \in [p]$ and $t \in \mathbb{R}$, denote

$$\begin{aligned} \widehat{G}_{p,j}^0(t) &= \frac{1}{|ne_j^c|} \sum_{i \in ne_j^c} \mathbb{1}(M_{ji} > t), & \widehat{V}_{p,j}^0(t) &= \frac{1}{|ne_j^c|} \sum_{i \in ne_j^c} \mathbb{1}(M_{ji} < -t), \\ \widehat{G}_{p,j}^1(t) &= \frac{1}{|ne_j|} \sum_{i \in ne_j} \mathbb{1}(M_{ji} > t), & G_{p,j}^0(t) &= \frac{1}{|ne_j^c|} \sum_{i \in ne_j^c} \mathbb{P}(M_{ji} > t). \end{aligned} \quad (25)$$

Let $\pi_{p,j}^0 = |ne_j^c|/\sum_{j=1}^p |ne_j^c|$, $\pi_{p,j}^1 = |ne_j|/\sum_{j=1}^p |ne_j|$, and $r_{p,j} = \sum_{j=1}^p |ne_j|/\sum_{j=1}^p |ne_j^c|$. In addition, denote

$$\begin{aligned} \text{FDP}_p(t_1, \dots, t_p) &= \frac{\sum_{j=1}^p \pi_{p,j}^0 \widehat{G}_{p,j}^0(t_j)}{\sum_{j=1}^p \pi_{p,j}^0 \widehat{G}_{p,j}^0(t_j) + r_{p,j} \sum_{j=1}^p \pi_{p,j}^1 \widehat{G}_{p,j}^1(t_j)}, \\ \text{FDP}_p^\dagger(t_1, \dots, t_p) &= \frac{\sum_{j=1}^p \pi_{p,j}^0 \widehat{V}_{p,j}^0(t_j)}{\sum_{j=1}^p \pi_{p,j}^0 \widehat{G}_{p,j}^0(t_j) + r_{p,j} \sum_{j=1}^p \pi_{p,j}^1 \widehat{G}_{p,j}^1(t_j)}, \\ \overline{\text{FDP}}_p(t_1, \dots, t_p) &= \frac{\sum_{j=1}^p \pi_{p,j}^0 G_{p,j}^0(t_j)}{\sum_{j=1}^p \pi_{p,j}^0 G_{p,j}^0(t_j) + r_{p,j} \sum_{j=1}^p \pi_{p,j}^1 \widehat{G}_{p,j}^1(t_j)}. \end{aligned} \quad (26)$$

Lemma 4 Under Assumption 5, as $p \rightarrow \infty$, we have

$$\begin{aligned} \sup_{t_1, \dots, t_p} \left| \sum_{j=1}^p \pi_{p,j}^0 \left(\widehat{G}_{p,j}^0(t_j) - G_{p,j}^0(t_j) \right) \right| &\rightarrow 0 \quad \text{in probability,} \\ \sup_{t_1, \dots, t_p} \left| \sum_{j=1}^p \pi_{p,j}^0 \left(\widehat{V}_{p,j}^0(t_j) - G_{p,j}^0(t_j) \right) \right| &\rightarrow 0 \quad \text{in probability.} \end{aligned} \quad (27)$$

Proof of Lemma 4. For any $j \in [p]$, we first show that in probability, $\sup_t |\widehat{G}_{p,j}^0(t) - G_{p,j}^0(t)|$ converges to 0 as $p \rightarrow \infty$ exponentially fast. For any $\epsilon \in (0, 1)$, denote $-\infty = \alpha_0^{p,j} < \alpha_1^{p,j} < \dots < \alpha_{N_\epsilon}^{p,j} = \infty$ in which $N_\epsilon = \lceil 2/\epsilon \rceil$, such that $G_{p,j}^0(\alpha_{k-1}^{p,j}) - G_{p,j}^0(\alpha_k^{p,j}) \leq \epsilon/2$ for $k \in [N_\epsilon]$. We have

$$\begin{aligned} \mathbb{P} \left(\sup_t \widehat{G}_{p,j}^0(t) - G_{p,j}^0(t) > \epsilon \right) &\leq \mathbb{P} \left(\bigcup_{k=1}^{N_\epsilon} \sup_{t \in [\alpha_{k-1}^{p,j}, \alpha_k^{p,j})} \widehat{G}_{p,j}^0(t) - G_{p,j}^0(t) > \epsilon \right) \\ &\leq \sum_{k=1}^{N_\epsilon} \mathbb{P} \left(\sup_{t \in [\alpha_{k-1}^{p,j}, \alpha_k^{p,j})} \widehat{G}_{p,j}^0(t) - G_{p,j}^0(t) > \epsilon \right). \end{aligned} \quad (28)$$

We note that both $\widehat{G}_{p,j}^0(t)$ and $G_{p,j}^0(t)$ are monotonic decreasing function. Therefore, for any $k \in [N_\epsilon]$, we have

$$\sup_{t \in [\alpha_{k-1}^{p,j}, \alpha_k^{p,j})} \widehat{G}_{p,j}^0(t) - G_{p,j}^0(t) \leq \widehat{G}_{p,j}^0(\alpha_{k-1}^{p,j}) - G_{p,j}^0(\alpha_k^{p,j}) \leq \widehat{G}_{p,j}^0(\alpha_{k-1}^{p,j}) - G_{p,j}^0(\alpha_{k-1}^{p,j}) + \epsilon/2. \quad (29)$$

Based on Equation (28), Assumption 5(a), and the Azuma-Hoeffding inequality, it follows that

$$\mathbb{P} \left(\sup_t \widehat{G}_{p,j}^0(t) - G_{p,j}^0(t) > \epsilon \right) \leq \sum_{k=1}^{N_\epsilon} \mathbb{P} \left(\widehat{G}_{p,j}^0(\alpha_{k-1}^{p,j}) - G_{p,j}^0(\alpha_{k-1}^{p,j}) > \frac{\epsilon}{2} \right) \leq N_\epsilon \exp(-C|ne_j^c|^{1-2\alpha}\epsilon^2) \quad (30)$$

for some constant $C > 0$. Similarly, we can show that

$$\mathbb{P} \left(\inf_t \widehat{G}_{p,j}^0(t) - G_{p,j}^0(t) < -\epsilon \right) \leq \sum_{k=1}^{N_\epsilon} \mathbb{P} \left(\widehat{G}_{p,j}^0(\alpha_k^{p,j}) - G_{p,j}^0(\alpha_k^{p,j}) < -\frac{\epsilon}{2} \right) \leq N_\epsilon \exp(-C|ne_j^c|^{1-2\alpha}\epsilon^2). \quad (31)$$

It follows that

$$\begin{aligned} \mathbb{P} \left(\sup_{t_1, \dots, t_p} \left| \sum_{j=1}^p \pi_{p,j}^0 \left(\widehat{G}_{p,j}^0(t_j) - G_{p,j}^0(t_j) \right) \right| > \epsilon \right) &\leq \mathbb{P} \left(\bigcup_{j=1}^p \sup_{t_j \in \mathbb{R}} \left| \widehat{G}_{p,j}^0(t_j) - G_{p,j}^0(t_j) \right| > \epsilon \right) \\ &\leq \sum_{j=1}^p \mathbb{P} \left(\sup_{t \in \mathbb{R}} \left| \widehat{G}_{p,j}^0(t) - G_{p,j}^0(t) \right| > \epsilon \right) \leq 2N_\epsilon \sum_{j=1}^p \exp(-C|ne_j^c|^{1-2\alpha}\epsilon^2) \\ &\leq 2N_\epsilon p \exp \left(-C \min_{j \in [p]} |ne_j^c|^{1-2\alpha}\epsilon^2 \right) \rightarrow 0, \quad p \rightarrow \infty, \end{aligned} \quad (32)$$

under Assumption 5(b). The second convergence statement involves $\widehat{V}_{p,j}^0(t)$ can be shown similarly. This concludes the proof of Lemma 4.

Proof of Proposition 5. Following Equation (7), we have

$$\begin{aligned}
\limsup_{p \rightarrow \infty} \text{FDR} &\leq \limsup_{p \rightarrow \infty} 2\mathbb{E} \left[\text{FDP}_p \left(\tau_{q/2}^1, \dots, \tau_{q/2}^p \right) \right] \\
&\leq \limsup_{p \rightarrow \infty} 2\mathbb{E} \left| \text{FDP}_p \left(\tau_{q/2}^1, \dots, \tau_{q/2}^p \right) - \overline{\text{FDP}}_p \left(\tau_{q/2}^1, \dots, \tau_{q/2}^p \right) \right| \\
&\quad + \limsup_{p \rightarrow \infty} 2\mathbb{E} \left| \text{FDP}_p^\dagger \left(\tau_{q/2}^1, \dots, \tau_{q/2}^p \right) - \overline{\text{FDP}}_p \left(\tau_{q/2}^1, \dots, \tau_{q/2}^p \right) \right| \\
&\quad + \limsup_{p \rightarrow \infty} 2\mathbb{E} \left[\text{FDP}_p^\dagger \left(\tau_{q/2}^1, \dots, \tau_{q/2}^p \right) \right] \\
&\leq \limsup_{p \rightarrow \infty} 2\mathbb{E} \left[\sup_{t_1, \dots, t_p > 0} \left| \text{FDP}_p(t_1, \dots, t_p) - \overline{\text{FDP}}_p(t_1, \dots, t_p) \right| \right] \\
&\quad + \limsup_{p \rightarrow \infty} 2\mathbb{E} \left[\sup_{t_1, \dots, t_p > 0} \left| \text{FDP}_p^\dagger(t_1, \dots, t_p) - \overline{\text{FDP}}_p(t_1, \dots, t_p) \right| \right] \\
&\quad + \limsup_{p \rightarrow \infty} 2\mathbb{E} \left[\text{FDP}_p^\dagger \left(\tau_{q/2}^1, \dots, \tau_{q/2}^p \right) \right].
\end{aligned} \tag{33}$$

The first two terms are 0 based on Lemma 4 and the dominated convergence theorem. For the last term, we have

$$\limsup_{p \rightarrow \infty} 2\mathbb{E} \left[\text{FDP}_p^\dagger \left(\tau_{q/2}^1, \dots, \tau_{q/2}^p \right) \right] \leq \limsup_{p \rightarrow \infty} 2\mathbb{E} \left[\max_{j \in [p]} \frac{\#\{i \in ne_j^c, M_{ji} < -\tau_{q/2}^j\}}{\#\{M_{ji} > \tau_{q/2}^j\} \vee 1} \right] \leq q \tag{34}$$

based on the definition of $\tau_{q/2}^j$. This concludes the proof of Proposition 5.

6.2 Symmetrization of the Lasso estimator

We detail the variance σ_j^2 and the truncation points a_j, b_j discussed in Section 3.1, which essentially follow Lee et al. (2016). First, for notational convenience, we drop the dependency on the splitting index, and denote $\mathbf{X} = \mathbf{X}^{(1)}$, $\widehat{S}^{(1)} = \widehat{S}$. The variance is $\sigma_j^2 = \sigma^2 \mathbf{e}_j^\top \left(\mathbf{X}_{\widehat{S}}^\top \mathbf{X}_{\widehat{S}} \right)^{-1} \mathbf{e}_j$. Let $\mathbf{X}_{\widehat{S}}^+ = \left(\mathbf{X}_{\widehat{S}}^\top \mathbf{X}_{\widehat{S}} \right)^{-1} \mathbf{X}_{\widehat{S}}^\top$, $\boldsymbol{\eta} = \left(\mathbf{X}_{\widehat{S}}^+ \right)^\top \mathbf{e}_j$, and $\mathbf{z} = (I_n - P_{\boldsymbol{\eta}}) \mathbf{y}$, where $P_{\boldsymbol{\eta}}$ is the projection matrix onto $\boldsymbol{\eta}$. Let $\mathbf{c} = \boldsymbol{\eta}(\boldsymbol{\eta}^\top \boldsymbol{\eta})^{-1}$, \mathbf{s} be the sign of the original Lasso estimator, and

$$A = \begin{pmatrix} A_0(\widehat{S}, \mathbf{s}) \\ A_1(\widehat{S}, \mathbf{s}) \end{pmatrix}, \quad \mathbf{b} = \begin{pmatrix} \mathbf{b}_0(\widehat{S}, \mathbf{s}) \\ \mathbf{b}_1(\widehat{S}, \mathbf{s}) \end{pmatrix} \tag{35}$$

where

$$\begin{aligned}
A_0(\widehat{S}, \mathbf{s}) &= \frac{1}{\lambda} \begin{pmatrix} \mathbf{X}_{-\widehat{S}}^\top (I - P_{\widehat{S}}) \\ -\mathbf{X}_{-\widehat{S}}^\top (I - P_{\widehat{S}}) \end{pmatrix}, & \mathbf{b}_0(\widehat{S}, \mathbf{s}) &= \begin{pmatrix} 1 - \mathbf{X}_{-\widehat{S}}^\top (\mathbf{X}_{\widehat{S}}^+)^\top \mathbf{s} \\ 1 + \mathbf{X}_{-\widehat{S}}^\top (\mathbf{X}_{\widehat{S}}^+)^\top \mathbf{s} \end{pmatrix} \\
A_1(\widehat{S}, \mathbf{s}) &= -\text{diag}(\mathbf{s}) \left(\mathbf{X}_{\widehat{S}}^\top \mathbf{X}_{\widehat{S}} \right)^{-1} \mathbf{X}_{\widehat{S}}^\top, & \mathbf{b}_1(\widehat{S}, \mathbf{s}) &= -\lambda \text{diag}(\mathbf{s}) \left(\mathbf{X}_{\widehat{S}}^\top \mathbf{X}_{\widehat{S}} \right)^{-1} \mathbf{s}.
\end{aligned} \tag{36}$$

The truncation point a_j and b_j are as below:

$$a_j = \max_{k: (A\mathbf{c})_k < 0} \frac{b_k - (A\mathbf{z})_k}{(A\mathbf{c})_k}, \quad b_j = \max_{k: (A\mathbf{c})_k > 0} \frac{b_k - (A\mathbf{z})_k}{(A\mathbf{c})_k}. \tag{37}$$

6.3 Simulation details

6.3.1 Linear model

Methods	$\rho = 0.0$		$\rho = 0.2$		$\rho = 0.4$		$\rho = 0.6$		$\rho = 0.8$	
	FDR	Power								
($p = 500$)										
DS	0.10	0.83	0.10	0.81	0.07	0.80	0.10	0.73	0.11	0.58
MDS	0.04	0.86	0.04	0.86	0.05	0.83	0.05	0.77	0.06	0.67
M-knockoff	0.10	0.88	0.07	0.84	0.04	0.74	0.02	0.61	0.02	0.51
F -knockoff	0.09	0.84	0.10	0.85	0.09	0.82	0.10	0.76	0.11	0.62
BHq	0.06	0.81	0.06	0.80	0.06	0.77	0.09	0.72	0.08	0.61
BYq	0.01	0.76	0.01	0.72	0.01	0.73	0.01	0.67	0.02	0.55
MBHq	0.00	0.82	0.00	0.80	0.00	0.77	0.00	0.71	0.00	0.57
MBYq	0.00	0.82	0.00	0.79	0.00	0.77	0.00	0.71	0.00	0.58
($p = 1000$)										
DS	0.10	0.82	0.09	0.78	0.10	0.76	0.09	0.72	0.08	0.56
MDS	0.04	0.86	0.06	0.85	0.06	0.83	0.06	0.78	0.07	0.66
M-Knockoff	0.13	0.90	0.07	0.79	0.00	0.28	0.00	0.26	0.00	0.26
F -Knockoff	0.10	0.84	0.10	0.83	0.11	0.81	0.10	0.77	0.09	0.64
BHq	0.06	0.81	0.07	0.79	0.07	0.77	0.09	0.70	0.09	0.60
BYq	0.02	0.76	0.01	0.73	0.01	0.71	0.01	0.66	0.01	0.54
MBHq	0.00	0.82	0.00	0.80	0.00	0.78	0.00	0.73	0.00	0.58
MBYq	0.00	0.81	0.00	0.80	0.00	0.78	0.00	0.73	0.00	0.57
($p = 1500$)										
DS	0.10	0.74	0.10	0.72	0.10	0.67	0.10	0.62	0.11	0.51
MDS	0.07	0.81	0.06	0.81	0.08	0.77	0.09	0.73	0.09	0.60
M-Knockoff	0.11	0.86	0.03	0.68	0.00	0.16	0.00	0.09	0.00	0.08
F -Knockoff	0.11	0.79	0.11	0.78	0.12	0.74	0.13	0.70	0.12	0.58
BHq	0.07	0.74	0.07	0.72	0.11	0.67	0.05	0.64	0.08	0.52
BYq	0.01	0.68	0.01	0.66	0.03	0.61	0.01	0.58	0.01	0.45
MBHq	0.00	0.77	0.00	0.76	0.00	0.72	0.00	0.66	0.00	0.53
MBYq	0.00	0.77	0.00	0.76	0.00	0.72	0.00	0.66	0.00	0.53
($p = 2000$)										
DS	0.08	0.69	0.10	0.69	0.08	0.64	0.11	0.56	0.10	0.45
MDS	0.07	0.78	0.05	0.78	0.07	0.74	0.06	0.69	0.07	0.58
M-Knockoff	0.12	0.86	0.02	0.62	0.00	0.15	0.00	0.08	0.00	0.05
F -Knockoff	0.09	0.74	0.13	0.76	0.09	0.71	0.12	0.67	0.13	0.57
BHq	0.08	0.68	0.05	0.68	0.08	0.64	0.08	0.60	0.07	0.50
BYq	0.02	0.61	0.00	0.63	0.01	0.59	0.01	0.54	0.02	0.44
MBHq	0.00	0.75	0.00	0.74	0.00	0.70	0.00	0.64	0.00	0.53
MBYq	0.00	0.75	0.00	0.73	0.00	0.69	0.00	0.63	0.00	0.52

Table 1: Empirical FDRs and powers on the linear model, where the design matrix has pairwise constant correlation ρ . The number of true features is 50 across all settings. The signal-to-noise ratio is $10 \times \sqrt{\log p/n}$. The designated FDR control level is $q = 0.1$. The eight methods are, the single data-splitting method (DS), the multiple data-splitting method (MDS), the model-X knockoff filter (M-Knockoff), the fixed-design knockoff filter with data recycling (F-Knockoff), the Benjamini-Hochberg method (BHq) and its multiple data-splitting version (MBHq), the Benjamini-Yekutieli method (BYq) and its multiple data-splitting version (MBYq). The reported results are the empirical means of 50 independent runs.

SNR	$4\sqrt{\log p/n}$		$8\sqrt{\log p/n}$		$12\sqrt{\log p/n}$		$16\sqrt{\log p/n}$		$20\sqrt{\log p/n}$	
$(p = 500)$	FDR	Power	FDR	Power	FDR	Power	FDR	Power	FDR	Power
DS	0.10	0.48	0.09	0.70	0.10	0.78	0.10	0.82	0.09	0.84
MDS	0.09	0.59	0.06	0.76	0.05	0.83	0.04	0.86	0.04	0.87
M-Knockoff	0.00	0.30	0.01	0.59	0.03	0.73	0.03	0.78	0.05	0.82
F -Knockoff	0.10	0.56	0.10	0.74	0.09	0.82	0.09	0.85	0.09	0.87
BHq	0.07	0.45	0.07	0.69	0.07	0.78	0.05	0.83	0.06	0.86
BYq	0.01	0.36	0.01	0.62	0.01	0.74	0.01	0.80	0.01	0.84
MBHq	0.00	0.45	0.00	0.68	0.00	0.77	0.00	0.82	0.00	0.85
MBYq	0.00	0.44	0.00	0.68	0.00	0.77	0.00	0.82	0.00	0.85
<hr/>										
$(p = 1000)$	FDR	Power	FDR	Power	FDR	Power	FDR	Power	FDR	Power
DS	0.010	0.44	0.10	0.67	0.10	0.76	0.10	0.80	0.10	0.83
MDS	0.09	0.58	0.07	0.76	0.05	0.82	0.05	0.86	0.05	0.87
M-Knockoff	0.00	0.10	0.00	0.26	0.00	0.37	0.00	0.44	0.00	0.47
F -Knockoff	0.12	0.55	0.10	0.72	0.10	0.81	0.09	0.84	0.09	0.86
BHq	0.05	0.42	0.06	0.67	0.07	0.76	0.06	0.82	0.06	0.85
BYq	0.01	0.31	0.01	0.60	0.01	0.71	0.01	0.78	0.01	0.83
MBHq	0.00	0.44	0.00	0.68	0.00	0.77	0.00	0.83	0.00	0.85
MBYq	0.00	0.42	0.00	0.68	0.00	0.77	0.00	0.83	0.00	0.85
<hr/>										
$(p = 1500)$	FDR	Power	FDR	Power	FDR	Power	FDR	Power	FDR	Power
DS	0.10	0.40	0.09	0.62	0.10	0.70	0.10	0.74	0.10	0.77
MDS	0.09	0.54	0.09	0.72	0.07	0.79	0.06	0.82	0.05	0.84
M-Knockoff	0.00	0.05	0.00	0.11	0.00	0.16	0.00	0.19	0.00	0.25
F -Knockoff	0.15	0.53	0.12	0.70	0.10	0.76	0.11	0.79	0.10	0.81
BHq	0.08	0.38	0.07	0.62	0.06	0.72	0.06	0.78	0.05	0.81
BYq	0.01	0.29	0.01	0.56	0.01	0.66	0.01	0.74	0.01	0.78
MBHq	0.00	0.41	0.00	0.65	0.00	0.74	0.00	0.79	0.00	0.83
MBYq	0.00	0.40	0.00	0.65	0.00	0.74	0.00	0.79	0.00	0.83
<hr/>										
$(p = 2000)$	FDR	Power	FDR	Power	FDR	Power	FDR	Power	FDR	Power
DS	0.11	0.34	0.10	0.56	0.10	0.66	0.10	0.70	0.10	0.73
MDS	0.09	0.51	0.09	0.68	0.07	0.76	0.07	0.79	0.06	0.81
M-Knockoff	0.00	0.04	0.00	0.09	0.00	0.14	0.00	0.17	0.00	0.19
F -Knockoff	0.16	0.50	0.12	0.65	0.11	0.73	0.11	0.76	0.11	0.78
BHq	0.08	0.34	0.08	0.55	0.08	0.68	0.07	0.72	0.08	0.77
BYq	0.01	0.25	0.01	0.48	0.02	0.62	0.01	0.672	0.01	0.73
MBHq	0.00	0.39	0.00	0.61	0.00	0.71	0.00	0.77	0.00	0.80
MBYq	0.00	0.38	0.00	0.61	0.00	0.71	0.00	0.77	0.00	0.80

Table 2: Empirical FDRs and powers on the linear model, where the design matrix follows a multivariate normal distribution with constant pairwise correlation 0.5. SNR represents the signal-to-noise ratio. The number of true features is 50 across all settings. The designated FDR control level is $q = 0.1$. The eight methods are, the single data-splitting method (DS), the multiple data-splitting method (MDS), the model-X knockoff filter (M-Knockoff), the fixed-design knockoff filter with data recycling (F-Knockoff), the Benjamini-Hochberg method (BHq) and its multiple-splitting version (MBHq), the Benjamini-Yekutieli method (BYq) and its multiple-splitting version (MBYq). The reported results are the empirical means of 50 independent runs.

6.3.2 Deep neural network

Link function	$p = 500$		$p = 1000$		$p = 1500$		$p = 2000$		$p = 3000$	
	FDR	Power	FDR	Power	FDR	Power	FDR	Power	FDR	Power
$f_1(t)$										
DS-I	0.10	0.81	0.07	0.86	0.10	0.84	0.11	0.86	0.12	0.80
DS-II	0.07	0.80	0.10	0.83	0.11	0.82	0.14	0.86	0.11	0.80
MDS-I	0.05	0.79	0.03	0.83	0.06	0.82	0.07	0.85	0.08	0.79
MDS-II	0.02	0.78	0.07	0.86	0.09	0.84	0.07	0.85	0.09	0.82
DeepPINK-I	0.18	0.43	0.12	0.31	0.16	0.26	0.17	0.30	0.15	0.32
DeepPINK-II	0.14	0.41	0.15	0.24	0.13	0.17	0.12	0.17	0.14	0.13
$f_2(t)$										
DS-I	0.10	0.85	0.10	0.76	0.12	0.68	0.07	0.69	0.09	0.65
DS-II	0.10	0.87	0.09	0.72	0.11	0.66	0.08	0.67	0.08	0.62
MDS-I	0.05	0.83	0.06	0.74	0.08	0.66	0.05	0.67	0.06	0.63
MDS-II	0.05	0.84	0.04	0.71	0.07	0.65	0.04	0.64	0.05	0.61
DeepPINK-I	0.15	0.68	0.16	0.67	0.14	0.62	0.12	0.61	0.15	0.62
DeepPINK-II	0.11	0.59	0.10	0.61	0.18	0.56	0.14	0.59	0.07	0.54
$f_3(t)$										
DS-I	0.08	0.94	0.09	0.87	0.08	0.87	0.10	0.85	0.12	0.83
DS-II	0.10	0.96	0.10	0.89	0.10	0.88	0.11	0.87	0.13	0.83
MDS-I	0.04	0.90	0.06	0.84	0.05	0.84	0.06	0.82	0.06	0.80
MDS-II	0.04	0.92	0.05	0.86	0.07	0.85	0.07	0.84	0.09	0.81
DeepPINK-I	0.10	0.83	0.13	0.74	0.11	0.70	0.12	0.66	0.12	0.65
DeepPINK-II	0.09	0.88	0.09	0.84	0.14	0.83	0.12	0.79	0.10	0.68

Table 3: Empirical FDRs and powers on the single-index models. The design matrix follows multivariate normal distribution with pairwise power decay correlation. The five methods are, the single data-splitting method using the influence function (DS-I) and its multiple data-splitting version (MDS-I), the single data-splitting method using the weight multiplication (DS-II) and its multiple data-splitting version (MDS-II), and the DeepPINK method with two different network architectures (see the text for details). The designated FDR control level is $q = 0.1$ in all settings. The reported results are the empirical means of 20 independent runs.

Link function	$p = 500$		$p = 1000$		$p = 1500$		$p = 2000$		$p = 3000$	
	FDR	Power	FDR	Power	FDR	Power	FDR	Power	FDR	Power
$f_1(t)$										
DS-I	0.10	0.82	0.13	0.87	0.11	0.85	0.15	0.87	0.13	0.85
DS-II	0.09	0.83	0.13	0.87	0.09	0.84	0.14	0.87	0.13	0.85
MDS-I	0.06	0.80	0.07	0.84	0.08	0.83	0.08	0.87	0.07	0.84
MDS-II	0.05	0.81	0.06	0.86	0.04	0.82	0.06	0.86	0.07	0.84
DeepPINK-I	0.15	0.37	0.12	0.21	0.16	0.27	0.17	0.33	0.19	0.36
DeepPINK-II	0.13	0.41	0.14	0.23	0.12	0.18	0.11	0.16	0.16	0.13
$f_2(t)$										
DS-I	0.14	0.87	0.11	0.75	0.08	0.66	0.08	0.68	0.09	0.66
DS-II	0.11	0.85	0.07	0.71	0.07	0.66	0.08	0.66	0.09	0.64
MDS-I	0.08	0.85	0.07	0.73	0.05	0.64	0.04	0.65	0.05	0.64
MDS-II	0.04	0.83	0.05	0.68	0.06	0.64	0.05	0.64	0.05	0.62
DeepPINK-I	0.09	0.63	0.12	0.63	0.14	0.66	0.12	0.62	0.14	0.62
DeepPINK-II	0.07	0.61	0.11	0.64	0.17	0.65	0.09	0.64	0.12	0.58
$f_3(t)$										
DS-I	0.11	0.96	0.10	0.90	0.09	0.89	0.10	0.87	0.10	0.84
DS-II	0.10	0.98	0.08	0.89	0.11	0.89	0.09	0.88	0.09	0.84
MDS-I	0.05	0.94	0.05	0.87	0.04	0.85	0.05	0.83	0.06	0.80
MDS-II	0.03	0.95	0.05	0.86	0.07	0.85	0.06	0.85	0.05	0.81
DeepPINK-I	0.11	0.87	0.15	0.78	0.12	0.70	0.11	0.71	0.14	0.74
DeepPINK-II	0.10	0.90	0.13	0.86	0.12	0.85	0.09	0.79	0.13	0.72

Table 4: Empirical FDRs and powers on the single-index models based on 20 independent runs. The design matrix follows multivariate normal distribution with pairwise power decay partial correlation. The six methods are as per Figure 3. The designated FDR control level is $q = 0.1$ in all settings.

References

- Barber, R. F. and E. J. Candès (2015). Controlling the false discovery rate via knockoffs. *The Annals of Statistics* 43(5), 2055–2085.
- Barber, R. F. and E. J. Candès (2019). A knockoff filter for high-dimensional selective inference. *The Annals of Statistics* 47(5), 2504–2537.
- Benjamini, Y. and Y. Hochberg (1995). Controlling the false discovery rate: a practical and powerful approach to multiple testing. *Journal of the Royal Statistical Society: Series B (Statistical Methodology)* 57(1), 289–300.
- Benjamini, Y. and D. Yekutieli (2001). The control of the false discovery rate in multiple testing under dependency. *The Annals of Statistics* 29(4), 1165–1188.
- Bickel, P. J., Y. Ritov, and A. B. Tsybakov (2009). Simultaneous analysis of Lasso and Dantzig selector. *The Annals of Statistics* 37(4), 1705–1732.
- Candès, E., Y. Fan, L. Janson, and J. Lv (2018). Panning for gold: model-X knockoffs for high-dimensional controlled variable selection. *Journal of the Royal Statistical Society: Series B (Statistical Methodology)* 80(3), 551–577.
- Candès, E. and T. Tao (2007). The Dantzig selector: Statistical estimation when p is much larger than n . *The Annals of Statistics* 35(6), 2313–2351.
- Cox, D. R. (1975). A note on data-splitting for the evaluation of significance levels. *Biometrika* 62(2), 441–444.
- Dezeure, R., P. Bühlmann, L. Meier, and N. Meinshausen (2015). High-dimensional inference: confidence intervals, p -values and R-software hdi. *Statistical Science*, 533–558.
- Fan, J. and R. Li (2001). Variable selection via nonconcave penalized likelihood and its oracle properties. *Journal of the American statistical Association* 96(456), 1348–1360.
- Hechtlinger, Y. (2016). Interpretation of prediction models using the input gradient. *arXiv:1611.07634*.
- Ignatiadis, N., B. Klaus, J. B. Zaugg, and W. Huber (2016). Data-driven hypothesis weighting increases detection power in genome-scale multiple testing. *Nature methods* 13(7), 577.
- Katsevich, E. and C. Sabatti (2019). Multilayer knockoff filter: Controlled variable selection at multiple resolutions. *The Annals of Applied Statistics* 13(1), 1–33.
- Kim, S. (2015). ppcor: an R package for a fast calculation to semi-partial correlation coefficients. *Communications for Statistical Applications and Methods* 22(6), 665.
- Kingma, D. P. and J. Ba (2014). Adam: A method for stochastic optimization. *arXiv:1412.6980*.
- Lauritzen, S. L. (1996). Graphical models.
- Lee, J. D., D. L. Sun, Y. Sun, and J. E. Taylor (2016). Exact post-selection inference, with application to the Lasso. *The Annals of Statistics* 44(3), 907–927.
- Li, J. and M. H. Maathuis (2019). Nodewise knockoffs: False discovery rate control for Gaussian graphical models. *arXiv:1908.11611*.
- Liu, W. (2013). Gaussian graphical model estimation with false discovery rate control. *The Annals of Statistics* 41(6), 2948–2978.
- Lu, Y., Y. Fan, J. Lv, and W. S. Noble (2018). DeepPINK: reproducible feature selection in deep neural networks. In *Advances in Neural Information Processing Systems*, pp. 8676–8686.
- Meinshausen, N. and P. Bühlmann (2006). High-dimensional graphs and variable selection with the Lasso. *The Annals of Statistics* 34(3), 1436–1462.

- Meinshausen, N. and P. Bühlmann (2010). Stability selection. *Journal of the Royal Statistical Society: Series B (Statistical Methodology)* 72(4), 417–473.
- Meinshausen, N., L. Meier, and P. Bühlmann (2009). p-values for high-dimensional regression. *Journal of the American Statistical Association* 104(488), 1671–1681.
- Moran, P. A. P. (1973). Dividing a sample into two parts a statistical dilemma. *Sankhyā: The Indian Journal of Statistics, Series A*, 329–333.
- O’Hara, R. B. and M. J. Sillanpää (2009). A review of Bayesian variable selection methods: what, how and which. *Bayesian Analysis* 4(1), 85–117.
- Raskutti, G., M. J. Wainwright, and B. Yu (2010). Restricted eigenvalue properties for correlated Gaussian designs. *Journal of Machine Learning Research* 11(Aug), 2241–2259.
- Rhee, S. Y., W. J. Fessel, A. R. Zolopa, L. Hurley, T. Liu, J. Taylor, D. P. Nguyen, S. Slome, D. Klein, and M. Horberg (2005). HIV-1 protease and reverse-transcriptase mutations: correlations with antiretroviral therapy in subtype B isolates and implications for drug-resistance surveillance. *The Journal of Infectious Diseases* 192(3), 456–465.
- Rhee, S. Y., J. Taylor, G. Wadhwa, A. Ben-Hur, D. L. Brutlag, and R. W. Shafer (2006). Genotypic predictors of human immunodeficiency virus type 1 drug resistance. *Proceedings of the National Academy of Sciences* 103(46), 17355–17360.
- Rinaldo, A., L. Wasserman, M. G’Sell, and J. Lei (2016). Bootstrapping and sample splitting for high-dimensional, assumption-free inference. *arXiv:1611.05401*.
- Romano, J. P. and C. DiCiccio (2019). Multiple data splitting for testing.
- Rubin, D., S. Dudoit, and M. V. der Laan (2006). A method to increase the power of multiple testing procedures through sample splitting. *Statistical Applications in Genetics and Molecular Biology* 5(1).
- Stone, M. (1974). Cross-validated choice and assessment of statistical predictions. *Journal of the Royal Statistical Society: Series B (Statistical Methodology)* 36(2), 111–133.
- Storey, J. D., J. E. Taylor, and D. Siegmund (2004). Strong control, conservative point estimation and simultaneous conservative consistency of false discovery rates: a unified approach. *Journal of the Royal Statistical Society: Series B (Statistical Methodology)* 66(1), 187–205.
- Taylor, J., R. Lockhart, R. J. Tibshirani, and R. Tibshirani (2014). Exact post-selection inference for forward stepwise and least angle regression. *arXiv:1401.3889* 7, 10–1.
- Tibshirani, R. (1996). Regression shrinkage and selection via the Lasso. *Journal of the Royal Statistical Society: Series B (Statistical Methodology)* 58(1), 267–288.
- Tibshirani, R. J., J. Taylor, R. Lockhart, and R. Tibshirani (2016). Exact post-selection inference for sequential regression procedures. *Journal of the American Statistical Association* 111(514), 600–620.
- van de Wiel, M. A., J. Berkhof, and W. N. van Wieringen (2009). Testing the prediction error difference between 2 predictors. *Biostatistics* 10(3), 550–560.
- Wasserman, L. and K. Roeder (2009). High-dimensional variable selection. *The Annals of Statistics* 37(5A), 2178.
- Xin, X., Z. Zhao, and J. S. Liu (2019). Controlling false discovery rate using Gaussian mirrors. *arXiv:1911.09761*.
- Zhang, R., Z. Ren, and W. Chen (2018). SILGGM: An extensive R package for efficient statistical inference in large-scale gene networks. *PLoS Computational Biology* 14(8), e1006369.
- Zou, H. and T. Hastie (2005). Regularization and variable selection via the elastic net. *Journal of the Royal Statistical Society: Series B (Statistical Methodology)* 67(2), 301–320.